약학박사학위논문

암 면역 억제적 환경에서 자연 살해 세포의 결핍 기전에 관한 연구

Study on mechanism of natural killer cell deficiency in the tumor immunosuppressive environment

2013년 8월

서울대학교 대학원
약학과 의약생명과학전공
박 영 준

약학박사학위논문

암 면역 억제적 환경에서 자연 살해 세포의 결핍 기전에 관한 연구

Study on mechanism of natural killer cell deficiency in the tumor immunosuppressive environment

2013년 8월

서울대학교 대학원
약학과 의약생명과학전공
박 영 준

암 면역 억제적 환경에서 자연 살해 세포의 결핍 기전에 관한 연구

Study on mechanism of natural killer cell deficiency in the tumor immunosuppressive environment

지도교수 강 창 율
이 논문을 약학박사학위논문으로 제출함
2012년 11월

서울대학교 대학원
약학과 의약생명과학전공
박 영 준

박영준의 박사학위논문을 인준함
2013년 8월

위 원 장 _____

부 위 원 장 _____

위 원 _____

위 원 _____

위 원 _____

Abstract

Study on mechanism of natural killer cell deficiency in the tumor immunosuppressive environment

Park, Young-Jun

Laboratory of Immunology

Pharmaceutical Bioscience

Department of Pharmacy

The Graduate School

Seoul National University

How myeloid-derived suppressor cells (MDSC) emerge in the tumor environment remains unclear. Here we report that GM-CSF can convert natural killer (NK) cells into MDSC. When transferred into tumor-bearing mice, adoptively transferred NK cells lost their NK-phenotype and were

converted into Ly6C^{high}Ly6G^{high} MDSC. This conversion was abolished by exposure to IL-2 either in vitro or in vivo. Notably, we found that of the four maturation stages based on CD11b/CD27 expression levels, only the CD11b^{high}CD27^{high} NK cells could be converted into CD11b^{+}Gr1^{+} MDSC ex vivo. Transfer of CD27^{high} NK cells from tumor-bearing mice into tumor-bearing recipients was associated with conversion to MDSC in a manner associated with reduced numbers of CD11b^{high}CD27^{high} and CD11b^{high}CD27^{low} NK cell populations in the recipients. Our results identify a pathway of MDSC development from immature NK cells in tumor-bearing hosts, providing new insights into how tumor cells modulate their host immune microenvironment to escape immune surveillance.

Keywords : myeloid-derived suppressor cell, natural killer cell, tumor microenvironment, IL-2, CD11b, CD27, GM-CSF

Student number : 2006-23438

Table of Contents

Abstract.....i

Table of Contents.....iii

List of Figures.....iv

Abbreviations vi

Introduction.....1

Materials and Methods.....3

Results.....10

Figures.....22

Discussion.....49

References.....56

국문 초록.....64

List of Figures

Figure 1. Inverse relationship between the percentage of Ly6C$^{neg/low}$ cells and MDSCs. 22

Figure 2. Ly6C$^{neg/low}$ cells are converted into MDSCs. 24

Figure 3. NK cells are converted into MDSCs 26

Figure 4. Only tumor CD49b^{+} cells, not CD4^{+} or CD8^{+} T cells or B cells, are converted into MDSCs 28

Figure 5. IL-2 reverses the suppressive activity of MDSCs converted from CD49b^{+} cells 29

Figure 6. IL-2 subverts immunosuppressive tumor environment 31

Figure 7. CD49b^{+} cells from tumor-bearing mice are more prone to conversion into MDSCs compared to naïve CD49b^{+} cells 32

Figure 8. There is no significant difference between NK cells from naïve and tumor-bearing mice 34

Figure 9. NK cells are decreased in tumor-bearing mice 36

Figure 10. 4 populations of conventional NK cells divided by maturation state 37

Figure 11. CD11b^{high}CD27^{high} conventional NK cells are converted into MDSCs 39

Figure 12. The efficiency of conversion is increased in $CD11b^{high}CD27^{high}$ $NKp46^{+}$ cells compared to $NKp46^{+}$ total cells 41

Figure 13. Conversion of $CD11b^{high}CD27^{high}$ NK cells into MDSCs leads to $CD11b^{high}CD27^{high}$ and $CD11b^{high}CD27^{low}$ NK cell reduction..... 43

Figure 14. Endogenous MDSCs have no impact on NK cell death during the maturation course 45

Figure 15. The conversion of $CD11b^{high}CD27^{high}$ NK cells into MDSCs was not influenced dramatically by CD27 ligands..... 47

Abbreviations

CD, cluster of differentiation

MDSCs, myeloid-derived suppressor cells

NK cells, natural killer cells

IFN-γ, interferon- γ

IL-2, interleukin-2

TNF-α, tumor necrosis factor-α

NKG2D, natural killer group 2 member D

NKp46, natural killer cell p46-related protein

H&E, hematoxylin and eosin

GM-CSF, granulocyte-macrophage colony-stimulating factor

G-CSF, granulocyte colony-stimulating factor

M-CSF, macrophage colony-stimulating factor

IL-1β, interleukin-1β

IL-6, interleukin-6

IL-4, interleukin-4

IL-10, interleukin-10

TGF-β, transforming growth factor-β

Ag, antigen

Ab, antibody

Arg1, arginase1

Nox2, NADPH oxidase 2

Nfil3, nuclear factor interleukin-3

Pu.1, purine rich box-1

PBMC, peripheral blood mononuclear cell

T-bet, T-box expressed in T cells

Eomes, eomesodermin

VLS, vascular leak syndrome

***i*NOS,** inducible nitric oxide synthase

CTL, cytotoxic T lymphocyte

i.p*, intraperitoneally*

i.v*, intravenously*

s.c*, subcutaneously*

OVA, ovalbumin

FACS, fluorescence activated cell sorter

Mo, monocytic

PMN, polymorphonuclear

NF-κB, nuclear factor-κB

C/EBP, CCAAT-binding protein

FSC, forward scatter

SSC, side scatter

Study on mechanism of natural killer cell deficiency in the tumor immunosuppressive environment

Introduction

The tumor environment recruits diverse suppressor cells, such as M2 macrophages, regulatory T cells and MDSCs [1-3], to help cancer cells evade the attack by effector cells, leading to the subversion of the immune surveillance [3]. Of the suppressor cells, MDSCs comprise a mixed population of immature myeloid cells that accumulate in various pathological conditions, particularly in tumors. Recently, the morphological heterogeneity of MDSCs has been classified by the expression of Ly6C and Ly6G molecules, which has led to the identification of two MDSC subsets, i.e., $CD11b^{+}Ly6G^{+}Ly6C^{low}$ polymorphonuclear (PMN)-MDSCs and $CD11b^{+}Ly6G^{-}Ly6C^{high}$ monocytic (Mo)-MDSCs [4]. MDSCs utilize multiple mechanisms to suppress the adaptive and innate immune systems, and increased numbers of MDSCs correlate with a poor prognosis in cancer patients [5,6]. Recent studies have shown that a small number of transcription factors regulate aberrant myelopoiesis, leading to MDSC expansion [7-9]. Despite the advances in the field, the MDSC

developmental pathway remains in part elusive.

Contrast to MDSCs, NK cells present barriers to various tumors [10]. NK cell depletion leads to enhanced tumor growth in a mouse tumor model, indicating clearly the involvement of NK cells in tumor surveillance [11]. In addition, it has been shown that improved disease prognosis is associated with the extent of NK cell infiltration in non-small-cell lung carcinomas and colorectal cancers [12]. However, in a number of cases, NK cells in the tumor environment exhibit maturation and functional defects, decreasing the absolute number of cells [13-15]. Although a number of studies are underway to determine the cause of NK cell abnormalities, further investigations will be required.

In this study, we describe the unprecedented phenomenon that conventional NK cells in a specific maturation state in the tumor environment are converted into MDSCs in tumor-bearing mice. The number of NK cells decreased significantly as the implanted tumor grows, which may be attributed to the conversion of $CD11b^{high}CD27^{high}$ NK cells into MDSCs rather than being matured into $CD11b^{high}CD27^{low}$ phenotype. NK cell-activating cytokine IL-2 inhibited the development of MDSCs from NK cells *in vitro* and *in vivo*. Overall, *in vivo* IL-2 treatment induced NK cell expansion and augmented the activity of the cells, may result in the regression of tumor growth.

Materials and Methods

Mice and cell lines

All experiments were approved by the institutional Animal Care and Use Committee of Seoul National University. Six-week-old BALB/c, C57BL/6 mice were purchased from Charles River Laboratories and C57BL/6 CD45.1 congenic mice were purchased from JAX. The mice were bred and maintained in the Animal Facility for Pharmaceutical Research at Seoul National University under specific pathogen-free conditions.

CT26 colon adenocarcinoma cell line, EL4 lymphoma cell line and TC-1 lung carcinoma were obtained from the American Type Culture Collection (ATCC). Human Her-2/neu–expressing transfectoma Her2/CT26 cells were developed by transduction of CT26 using a retroviral vector system [16,17]. Cells were maintained in DMEM or RPMI 1640 medium supplemented with 10% heat-inactivated fetal bovine serum, 1% penicillin-streptomycin (G418 was supplemented for transfectoma). Cell lines were periodically authenticated by morphologic inspection and passaged for no more than 3-4 weeks from thawing.

Antibodies and flow cytometry

Anti-CD11b, CD27-APC, anti-Ly6G-PE/Cy7 (BioLegend), anti-F4/80, CD4 (eBioscience), CD11c (BD Biosciences), CD14, CD49b, CD8, B220, NK1.1, NKp46-PE, anti-CD3, CD19, Gr1-PerCP/Cy5.5, anti-CD122, CD45.1, Ly6C-FITC, anti-CD45.2-PacificBlue (BioLegend) antibodies were used. IL-2 neutralizing Ab and IL-2 receptor β-blocking Ab were obtained from S4B6 and TMβ1 hybridomas, respectively, and were kind gifts from Charles D. Surh (Scripps Institute). IL-2 receptor α-blocking Ab, which was obtained from hybridoma PC61, was a kind gift from S. Sakaguchi (Osaka University). To analyze the stained cells, FACSCalibur (BD Biosciences) instrument and FlowJo (Treestar) were used.

***In vitro* T cell suppression assay**

The DO11.10 cells ($1x10^5$/well) were stimulated with OVA protein (grade V; Sigma-Aldrich) and were cocultured with or without cytokine-induced MDSCs for 72 hr. For the final 20-24 hr, we added 1 μCi/well [^{3}H]-thymidine. The incorporation of the [^{3}H]-thymidine into the divided cells was detected using a liquid scintillation counter (Wallac, Turku, Finland).

ROS production, arginase 1 activity and NO production

For ROS detection, cells were incubated in the presence of 2.5 μM DCFDA ± 30 ng/ml PMA for 30 min. The fluorescence intensity of DCFDA was analyzed by flow cytometry.

Cells were incubated with 2 ng/ml IFN-γ and 100 ng/ml LPS for 18 hr. To detect NO production, supernatants were collected and mixed with equal volumes of Greiss reagent (1% sulfanilamide in 5% phosphoric acid and 0.1% N-1-naphthylethylenediamine dihydrochloride in DW) after 10 min, the absorbance at 540 nm was measured. The concentrations were determined by the standard curve of serial dilution of sodium nitrite. Arginase 1 activity was measured in cell lysates (lysed with 0.1% Triton X-100). Subsequently, 50 μl of 10 mM $MnCl_2$, 50 mM Tris/HCl were added, and the enzyme was activated by heating for 10 min at 55°C. Arginine hydrolysis was conducted by incubating the lysates with 0.5 M arginine (pH 9.7) at 37 °C for 80 min. The reaction was stopped with 400 μl of acid mixture ($H_2SO_4/H_3PO_4/H_2O$ = 1/3/7). Urea production was measured at 540 nm after addition of 9% α-isonitrosopropiophenone (control Abs. subtracted from specific Abs.).

***In vivo* IL-2/αIL-2 Ab complex (IL-2 complex) treatment**

To verify the effect of IL-2 on MDSC accumulation and function *in vivo*, we used an IL-2 complex. Mice received an i.p. injection of 1.5 μg rmIL-2 plus 50 μg αIL-2 Ab. Before injection, rmIL-2 and the αIL-2 Ab were mixed and incubated at room temperature for 15 min.

Tumor model and isolation of tumor infiltrating lymphocytes

C57BL/6 mice were injected s.c. with $2x10^5$ TC-1 tumor cells. Injection of IL-2 complex began on day 1 after tumor injection. IL-2 complex treatment was administered every other day for a total of 5 or 10 times. The volume of the implanted tumor was evaluated for 19 days following the s.c. tumor inoculation. To separate the tumor-infiltrating lymphocytes, the tumors were collected and weighed and single-cell suspensions were prepared. The tumor was cut into small pieces and was incubated at 37℃ for 0.5 hr in RPMI 1640 containing 1 mg/ml collagenase (Roche), 500 μg/ml DNase I and 25 μg/ml hyaluronidase (Sigma, St. Louis, MO).

Cell sorting

To sort $CD49b^+$ cells, splenocytes were prepared from tumor-bearing mice. To enrich the desired cell population, $CD4^+$, $CD8^+$, $B220^+$ and $Ly6G^+$ cells were

depleted using microbeads (Miltenyi Biotec, Germany). $CD11b^{+}Ly6C^{neg/low}Ly6G^{-}CD49b^{+}$ cells were sorted by using FACSAria II. To sort the conventional NK cells, splenocytes were enriched by the depletion of CD4, CD8, CD19 and $Ly6G^{+}$ cells using microbeads. $CD3^{-}CD19^{-}Gr1^{-}CD122^{+}NK1.1^{+}$ /$NKp46^{+}$ cells were sorted.

***In vivo* conversion assay of NK cells**

To determine the conversion of NK cells *in vivo*, EL4 tumor cells were injected s.c. into CD45.2 mice. After 3 weeks, $2.5x10^{5}$ $CD27^{high}$ NK cells ($CD11b^{low}CD27^{high}$: $CD11b^{high}CD27^{high}$ = 1: 2) were isolated from the spleen and were transferred i.v. into CD45.1 naïve mice or mice that were inoculated s.c. with $1x10^{5}$ tumor cells 7 days before the adoptive transfer. On day 14 after the transfer, $CD45.2^{+}CD45.1^{-}$ cells were analyzed for the expression of NK cell and MDSC markers in the spleen. For conversion assay in i.p. tumor model, EL4 tumor cells were injected s.c. into CD45.1 congenic mice. After 3 weeks, $NK1.1^{+}$ cells were isolated from the spleen by FACS ARIA III and transferred i.p. into naïve mice (NK1.1->Naïve host) or mice that had been inoculated with $1x10^{6}$ EL4 tumor cells 5 days before the adoptive transfer (NK1.1->Tumor host), with a daily injection of IL-2 complex until sacrifice

(NK1.1->Tumor host+IL-2). On day 9 after the adoptive transfer, cells were collected from the peritoneal cavity and $CD45.1^{+}CD45.2^{-}$ cells were analyzed.

Quantitative real-time- PCR

Total RNA was extracted using the TRIzol reagent, and cDNA was generated with SuperScript reverse transcriptase and oligo(dT) primers (all from Invitrogen Life Technologies). The LightCycler optical system (Roche) and the SYBR green real-time PCR kit (Takara) were used for the analysis of gene expression. Target gene values were calculated relative to *hprt* expression. The following primer pairs were used:

Cd122 antisense (GGAACGACCCGAGGATCAG); *Cd116* sense (AACGTGACTGACAGG AAGG); *Cd116* antisense (TGTGTGTGCTGGCTGTTAAGG); *Cd131* sense (AAGAGCCTGCAACTCACTGGCAC); *Cd131* antisense (TGGGGGTTTGGCTCCACTCATCTT); *Cebpα* sense (CCCCAGTCAGACCAGAAAGC); *Cebpα* antisense (TGGTCCCCGTGTCCTCCTA); *Nfil3* sense (AAGGGCCCCATCCATTCTC); *Nfil3* antisense (TTCAAACTCGCTGTCCAAAGC); *Pu.1* sense

(GCCTCAGTCACCAGGTTTCC); *Pu.1* antisense (CTCTCACCCTCCTCCTCATCTG); *Hprt* sense (AAGACTTGCTCGAGATGTCATGAA); *Hprt* antisense (ATCCAGCAGGTCAGCAAAGAA).

Statistical analysis

Statistical analyses were performed using Student's t test. The results with values of $p<0.05$ were considered to be statistically significant.

Results

Inverse relationship between the percentage of $CD11b^{+}Ly6G^{-}Ly6C^{neg/low}$ cells and MDSCs reveals the conversion of NK-phenotype cells into MDSCs.

To explore the development of tumor-associated MDSC, we utilized animal models of Her-2-expressing CT26 colon carcinoma and EL4 thymoma. When these tumor cells were subcutaneously inoculated into mice, we observed that the percentage of $Ly6C^{neg/low}$ cells (R1) among $CD11b^{+}$ population gradually declined in the spleen during tumor progression (Figure 1A and B). In contrast, $Ly6G^{high}$ PMN-MDSCs (R2) and $Ly6C^{high}$ Mo-MDSCs (R3) significantly increased in tumor-bearing mice compared to those in naïve mice. This observation led us to hypothesize that the tumor environment promotes the conversion of $CD11b^{+}Ly6G^{-}Ly6C^{neg/low}$ cells into MDSCs. To address this hypothesis, we cultured $CD11b^{+}Ly6G^{-}Ly6C^{neg/low}$ cells with cytokines that are known to be relevant to MDSC accumulation [4], and found that most of the cytokines tested induced them to become $Ly6G^{high}$ and/or $Ly6C^{high}$ cells, although the extent varied depending on the cytokine used (Figure 2A). Considering the number of live converted cells and the proportions of $Ly6C^{high}/Ly6G^{high}$ cells after incubation, GM-CSF was the most efficient

cytokine at converting $Ly6C^{neg/low}$ cells into MDSCs *in vitro* (Figure 2 B and C).

Flow cytometric analysis revealed that the majority of $CD11b^{+}Ly6G^{-}$ $Ly6C^{neg/low}$ cells expressed CD49b, but not CD14, CD11c, CD4, CD8, and B220 (Figure 2D). Furthermore, FACS-sorted $CD49b^{+}$ cells (purity > 98%) obtained from tumor-bearing mice were converted into $Ly6G^{high}Ly6C^{high}$ MDSC-like cells upon stimulation with GM-CSF (data not shown). To directly ask if NK cells can be converted into MDSCs, we purely isolated $NK1.1^{+}$ and $CD49b^{+}NKp46^{+}$ cells from C57BL/6 and BALB/c mice, respectively, and stimulated them with GM-CSF. As depicted in Figure 3A, GM-CSF down-regulated the NK cell markers NK1.1, CD49b, and NKp46, but instead up-regulated the expression of MDSC markers Ly6C and Ly6G. Same treatment failed to induce Ly6C and Ly6G on $CD4^{+}$, $CD8^{+}$ T cells and B cells (Figure 4). Similarly, FACS-sorted $CD49b^{+}NKp46^{+}$ cells (purity > 95%) from the bone marrow were also converted into $Ly6G^{high}$ and $Ly6C^{high}$ cells in the presence of GM-CSF, which was accompanied by a decrease in NK-marker expression ($CD49b^{+}$, 40.5%; $NKp46^{+}$, 14.8%). However, $CD49b^{+}NKp46^{+}$ cells from the PBMC did not respond to GM-CSF stimulation (data not shown).

To further investigate the observed conversion of NK cells into MDSC-like

cells, we examined if IL-2 affects this process since this cytokine activates NK cells and potentiates NK cell-mediated anti-tumor activity. Notably, addition of IL-2 not only inhibited the expression of Ly6C and Ly6G triggered by GM-CSF, but also maintained the expression of NK cell markers NK1.1, CD49b and NKp46 (Figure 3A).

To further investigate the role of IL-2 *in vivo*, $NK1.1^+$ cells were isolated (purity > 97%, Figure 3B) from tumor-bearing CD45.1 mice and transferred into CD45.2 mice inoculated i.p. with tumor cells 5 days before the adoptive transfer. Donor cells from the peritoneal cavity were analyzed. Up to 66% of the transferred $Ly6C^{neg/low}NK1.1^+$ cells were converted into Ly6C and/or $Ly6G^{high}$ MDSCs, whereas only 20% of the cells retained $NK1.1^+$ phenotype (Figure 3C). When the recipients were additionally given CD122-biased IL-2/IL-2 neutralizing-Ab complex (IL-2 complex) [18,19], most of the transferred cells maintained NK cell phenotype (Ly6C and/or $Ly6G^{high}$, 3.6%; $NK1.1^+$, 99%). In addition, there was minimal conversion of $NK1.1^+$ cells in naïve recipients (Ly6C and/or $Ly6G^{high}$, 7%; $NK1.1^+$, 87.4%). Taken together, these results demonstrated that NK cells can be converted into MDSC-like cells in tumor-bearing host *in vivo*, or by tumor-associated cytokines including GM-CSF *ex vivo*, and IL-2 can inhibit this conversion.

IL-2 reverses the suppressive activity of MDSCs converted from NK-phenotype cells and subverts tumor environment.

To examine if the MDSC-like cells converted from NK cells possess immune-suppressive activity, we obtained the $Ly6C^{high}Ly6G^{high}$ cells converted from $CD49b^{+}$ cells after stimulation with GM-CSF, and co-cultured them with DO11.10 splenocytes whose T cell receptor recognizes OVA presented by MHC II. As shown in Figure 5B, addition of the MDSC-like cells significantly inhibited OVA-induced proliferation of DO11.10 T cells, which resembled the suppressive activity of purified PMN- and Mo-MDSCs (Figure 5A). However, IL-2 significantly reversed the suppressive activity of the converted $CD49b^{+}$ cells (Figure 5B). The converted cells also displayed ROS/NO production (Figure 5C and D) and arginase 1 activity (Figure 5E), by which MDSCs inhibit the immune response, but decreased level or not shown in IL-2/GM-CSF-treated or purified $CD49b^{+}$ cells, indicating that the $Ly6C^{high}Ly6G^{high}$ cells that originated from NK cells after GM-CSF stimulation were likely bona fide MDSC cells with suppressive activity as well as with MDSC-signature secretion profiles.

To analyze the effect of IL-2 on MDSC populations and tumor growth, mice were treated with IL-2 complex every other day after TC1 tumor inoculation.

The tumor growth was suppressed by IL-2 treatment (Figure 6A and B), as the proportion of MDSCs per tumor weight was reduced, although $NK1.1^+$ cells were increased among tumor infiltrating leukocytes (Figure 6C). However, IL-2 cessation re-accelerated the tumor growth, $Ly6C^{high}$ MDSCs were also replenished and, importantly, $NK1.1^+$ cells were decreased in the tumor bed (Figure 6C). In the spleen, the IL-2 counteracting effect on the frequency of MDSCs and NK cells was also prominent, although it did not have a significant effect on the cell numbers (Figure 6D and E). This can be explained by previous studies showing that IL-2 directly or indirectly enhances the survival of granulocytes and monocytes [20-22].

$CD49b^+$ cells are prone to conversion into MDSCs in the tumor environment.

To investigate whether the 'MDSC-philic' cytokine-induced conversion of NK-phenotype cell into MDSCs is a property acquired in response to environmental cues or is an inherited feature, $CD49b^+$ cells were isolated from naïve, 3- and 5-week tumor-bearing mice. The longer NK-phenotype cells remained in the tumor environment, the more likely they were to become $Ly6C/Ly6G^{high}$ MDSCs following cytokine treatment. $CD49b^+$ cells from the

naïve and 3-week tumor-bearing mice responded to GM-CSF; however, 50-60% of the cells remained $CD49b^+$ cells, and the amount of $CD49b^+$ cells from the 5-week tumor-bearing mice was reduced to 19% (Figure 7A). In addition, IL-2-mediated inhibition was less potent in $CD49b^+$ cells from the 5-week tumor-bearing mice than the 3-week tumor-bearing mice. This observation was confirmed by the increased induction of $CD49b^-$ population, which was 17% in the 5-week tumor-bearing mice and 7% in the 3-week tumor-bearing mice in the presence of GM-CSF and IL-2 (Figure 7A). These data indicate that NK cells may enter a conversion state that is biased toward MDSCs in the tumor environment.

The change in responsiveness to IL-2 was further demonstrated by analyzing the related-cytokine receptors. $CD49b^+$ cells from the 5-week tumor-bearing mice preferentially expressed GM-CSF receptor β-chain (CD131), whereas the expression of IL-2 receptor β-chain (CD122) was decreased compared to the expression in the naïve or the 3-week tumor-bearing mice. The expression of GM-CSF receptor α-chain (CD116) did not increase significantly in the 5-week tumor-bearing mice (Figure 7B). Although the expression of *Nfil3*, an essential regulator of NK cell development [23,24], was decreased, the expression levels of *Cebpα* and *Pu.1*, essential transcription factors for granulocyte and

monocyte development [25,26], were significantly increased in CD49b^{+} cells from the 5-week tumor-bearing mice compared to the naïve mice (Figure 7B). To delineate whether the conversion was driven by these transcription factors, we analyzed the kinetics of gene expression during the cytokine stimulation. The expression of both genes was significantly down-regulated, as early as 6 hr after IL-2/GM-CSF stimulation, compared to the stimulation with GM-CSF alone. The gap in the gene expression level was sustained at all the time points examined. The greatest difference was observed early for *Cebpα* expression and at a later time point for *Pu.1* (Figure 7C). These results suggest that the sustained expression of *Cebpα* and *Pu.1* in the presence of GM-CSF may drive the conversion of NK-phenotype cells. However, further investigation will be needed to provide direct evidence for this hypothesis.

CD11b^{high}CD27^{high} subset of NK cells is converted into MDSCs in tumor-bearing mice.

Despite prominent difference in the responsiveness to GM-CSF, we observed no significant difference in the expression of surface/transcription markers related to the lineage specification, NK cell receptors, the secretion of effector/suppressive cytokines between NK cells from naïve and tumor-

bearing mice (Figure 8). To provide more definitive evidence for which NK cells in the tumor environment were converted into MDSCs, we further analyzed the difference in the extent of NK cell maturation based on CD11b/CD27 expression [27] between the naïve and tumor-bearing mice. The numbers of total NK cells were significantly decreased in the spleen and bone marrow of the mice inoculated with tumor cells for 3 weeks compared with naïve mice (Figure 9A and B). Importantly, the numbers of $CD11b^{high}CD27^{high}$ and $CD11b^{high}CD27^{low}$ subsets among NK cells were significantly reduced in tumor-bearing mice compared with naïve mice, while those of the other subsets were relatively similar (Figures 9C and D).

To elucidate whether the reduction of those NK cell populations was attributed to the observed conversion, we separated the $lineage^-$ ($CD3^-CD19^-Gr1^-$) $CD122^+NKp46$ or $NK1.1^+$ cells from tumor-bearing mice into 4 stages based on CD11b/CD27 expression level (Figure 10A and B) and culture them in the presence of GM-CSF. Notably, $CD11b^{high}CD27^{high}$ NK cells obtained from tumor-bearing mice were converted into $CD11b^+Gr1^+$ MDSC phenotype (Figure 11A and B), whereas their naïve counterpart and $CD11b^{low}CD27^{low}$, $CD11b^{low}CD27^{high}$, $CD11b^{high}CD27^{low}$ NK cells from tumor-bearing mice hardly did (data not shown). Comparable purity of $CD122^+NKp46^+$ cells for

sorting showed that the unwanted cells were present equally (0.8-1.3%) in 4 sorted populations (Figure 10A), indicating that this phenomenon was not due to myeloid precursors in the tumor environment. Moreover, the GM-CSF-treated $CD11b^{high}CD27^{high}NKp46^{+}$ cells yielded a 3.6 fold greater number of converted cells compared to those from $NKp46^{+}$ cells (purity > 98.5 and 98.1%, respectively, Figure 12A and B). Furthermore, we evaluated the conversion efficiency based on the starting cell numbers. While the efficiency was only 2% in $NKp46^{+}$ cells, this increased to 10% in $CD11b^{high}CD27^{high}NKp46^{+}$ cells (Figure 12C), of which tendency was consistent with the proportion of $CD11b^{high}CD27^{high}$ population included in the purified $NKp46^{+}$ cells (Figure 12A, low panel). This discrepancy in which 'NK $maker^{-}$' cells equally included between NK populations indicates that the conversion arose from 'NK $marker^{+}$' cells. Annexin V staining revealed that 54% of the GM-CSF-treated $CD11b^{high}CD27^{high}NKp46^{+}$ cells were apoptotic during the course of conversion (Figure 12D).

The expression of CD122, NKp46 and NK1.1 was down-regulated in the presence of GM-CSF alone while retained in GM-CSF/IL-2 (Figure 11A and B). The morphology of the $CD11b^{high}CD27^{high}$ population was similar to the other populations of NK cells and the naïve $CD11b^{high}CD27^{high}$ NK cells,

which exhibited a shape consistent with lymphocytes (Figure 10C). In contrast, ring-, segmented band- and monocyte-shaped cells were observed after *in vitro* stimulation with GM-CSF. In the presence of GM-CSF/IL-2, the cells exhibited the morphology of activated NK cells (Figure 11C). Another NK-activating cytokine, IL-15, also exerted an inhibitory effect on conversion upon addition of low (20 ng/ml) and high (50 ng/ml) concentrations, although low levels of $CD11b^{+}Gr1^{+}$ cells (1.2%) were present after the addition of low concentration of IL-15 (Figure 11D).

To demonstrate this phenomenon *in vivo*, we purified $CD45.2^{+}CD27^{high}$ NK cells from tumor-bearing mice and transferred the cells into congenic CD45.1 mice. In tumor-bearing recipients, 12% of the transferred cells were converted into $CD11b^{+}Gr1^{+}$ MDSC phenotype (Figure 13A and B). In addition, the expression of CD122 and NK1.1 was decreased. In contrast, the phenotype of $CD27^{high}$ NK cells was retained in naïve recipients. Moreover, $CD11b^{high}CD27^{low}$ NK cells and $CD27^{high}$ NK cells from tumor-bearing and naïve mice, respectively, were rarely converted into MDSCs. Furthermore, the number of $CD11b^{high}CD27^{low}$ and $CD11b^{high}CD27^{high}$ NK cells that arose from transferred $CD27^{high}$ NK cells was reduced significantly in tumor-bearing recipients compared to naïve recipients (Figure 13C-E).

However, endogenous MDSCs may cause cell death of transferred $CD27^{high}$ NK cells, by which the matured NK cells were reduced. To investigate this, we evaluated the cell death of donor cells. The frequency of Annexin V^+ donor cells tended to increase in the tumor-bearing host compared to the naïve host, although the difference was not statistically significant (Figure 14A). To examine whether MDSCs rendered donor NK cells apoptotic, we transferred MDSCs ($4x10^6$/injection) into naive recipients 1 day before and after NK cell transfer. There was no difference in the frequency of apoptotic donor cells in the MDSC-treated naïve hosts compared to the naïve hosts (Figure 14A). In the same experimental setting, the donor cells were significantly more converted into MDSCs in the tumor-bearing hosts than in the naïve or MDSC-treated naïve hosts (Figure 14B). To more directly clarify the effect of MDSCs on NK cells during maturation, we stimulated $CD45.2^+$ $CD27^{high}$ NK cells with IL-12, -15 and -18 to mature them *in vitro* [28] (Figure 14C). These cytokines preferentially upregulated the expression of KLRG1 and CD11b, maturation markers for NK cells, compared to the untreated NK cells. However, no differences were observed in the maturation and apoptosis of NK cells even when $CD45.1^+$MDSCs were added 3 or 6 times compared to other conditions. These results suggested that the reduction of NK cells could be

attributed to their conversion into MDSCs, and possibly cell death, in the tumor environment. However, the viability and maturation of NK cells did not seem to be influenced by endogenous MDSCs, at least in the EL4 tumor model.

Figures

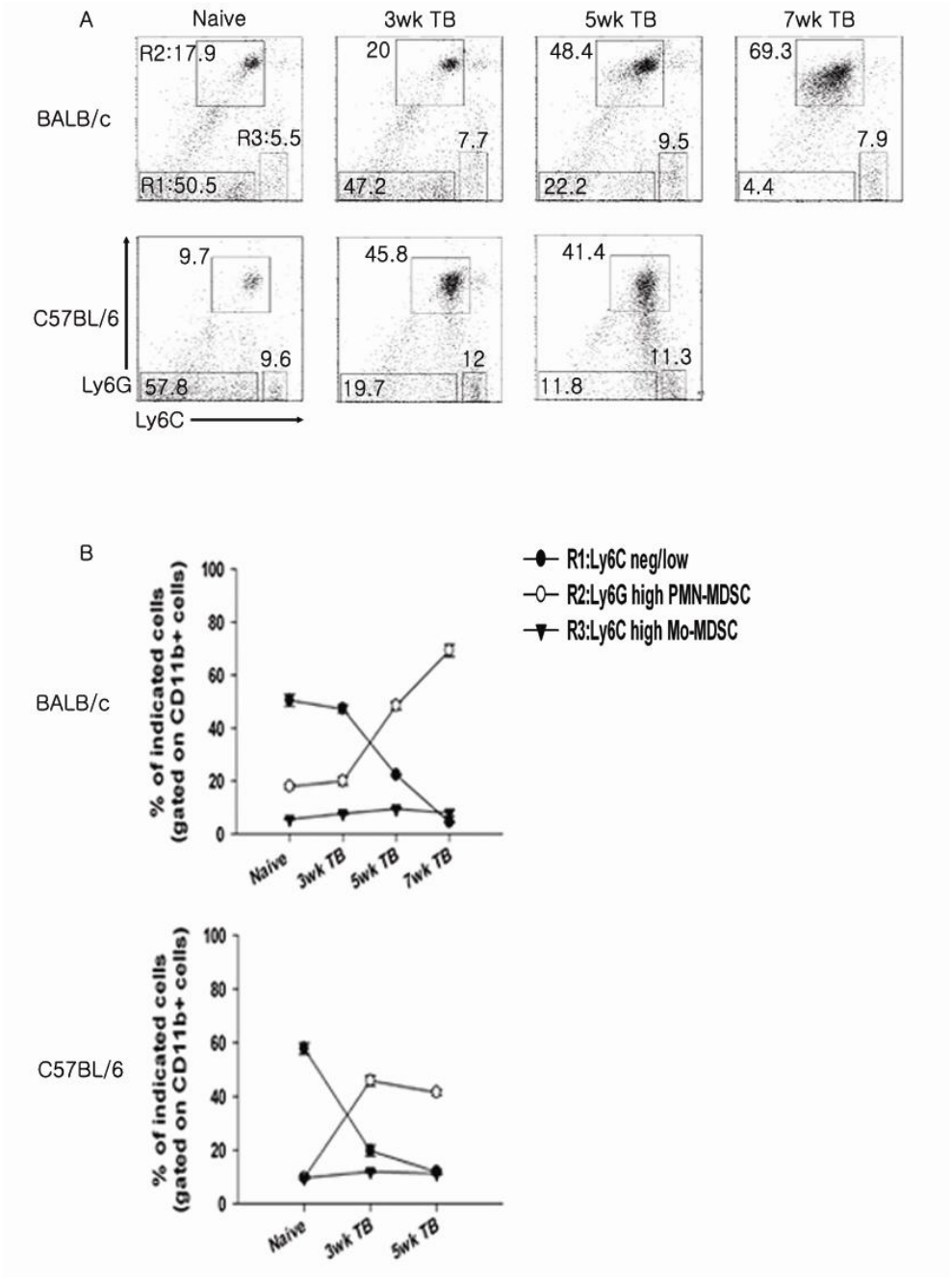

Figure 1. Inverse relationship between the percentage of Ly6C$^{neg/low}$ cells and MDSCs.

BALB/c or C57BL/6 mice were injected s.c. with $1x10^5$ Her-2/CT26 or EL4 tumor cells, respectively. The mice were euthanized at 3, 5 or 7 weeks after tumor inoculation.

(A) The various cell populations were classified by their Ly6C and Ly6G expression pattern within $CD11b^+$ cells in the spleen. The numbers in the plot indicate the percentage of gated cells. (B) The data represent the percentage (mean ± SEM) of indicated cell populations from the mice in (A) (3-4 mice per group). The data represent 3 independent experiments.

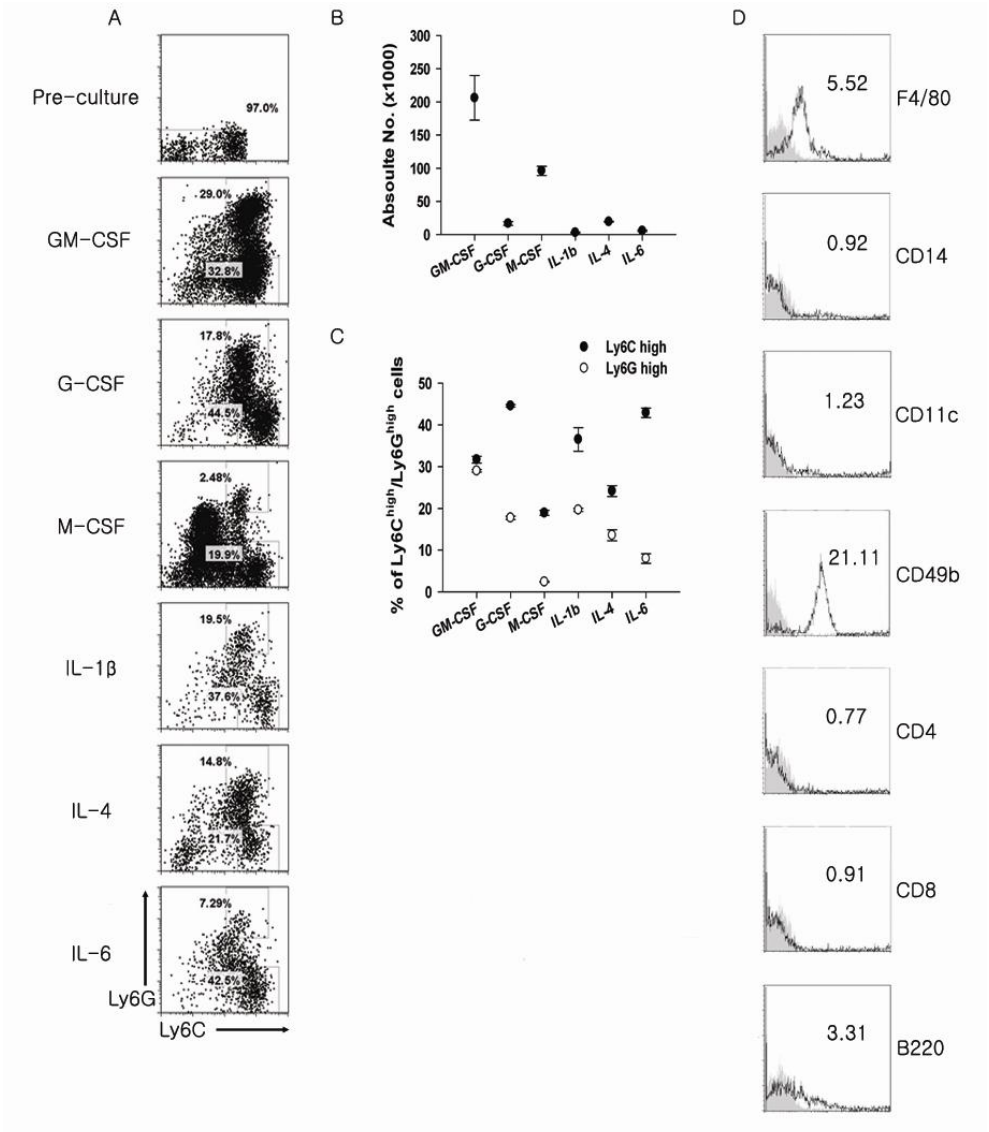

Figure 2. Ly6C$^{neg/low}$ cells are converted into MDSCs.

(A-B) Ly6C$^{neg/low}$ cells within CD11b^{+} cells were isolated from 3-week tumor-bearing C57BL/6 mice. These cells were incubated with 20 ng/ml of the indicated cytokines. On day 5, Ly6C/G expression was analyzed by FACS (A). The graphs indicate the number of live cells (B) and the percentage of

$Ly6C^{high}/Ly6G^{high}$ cells (C) after the incubation.

(D) $Ly6C^{neg/low}$ cells from the tumor-bearing mice were enriched and analyzed for the expression of lineage markers. Shaded, isotype control. The numbers in the plot indicate the geometric MFI ratio to isotype control .

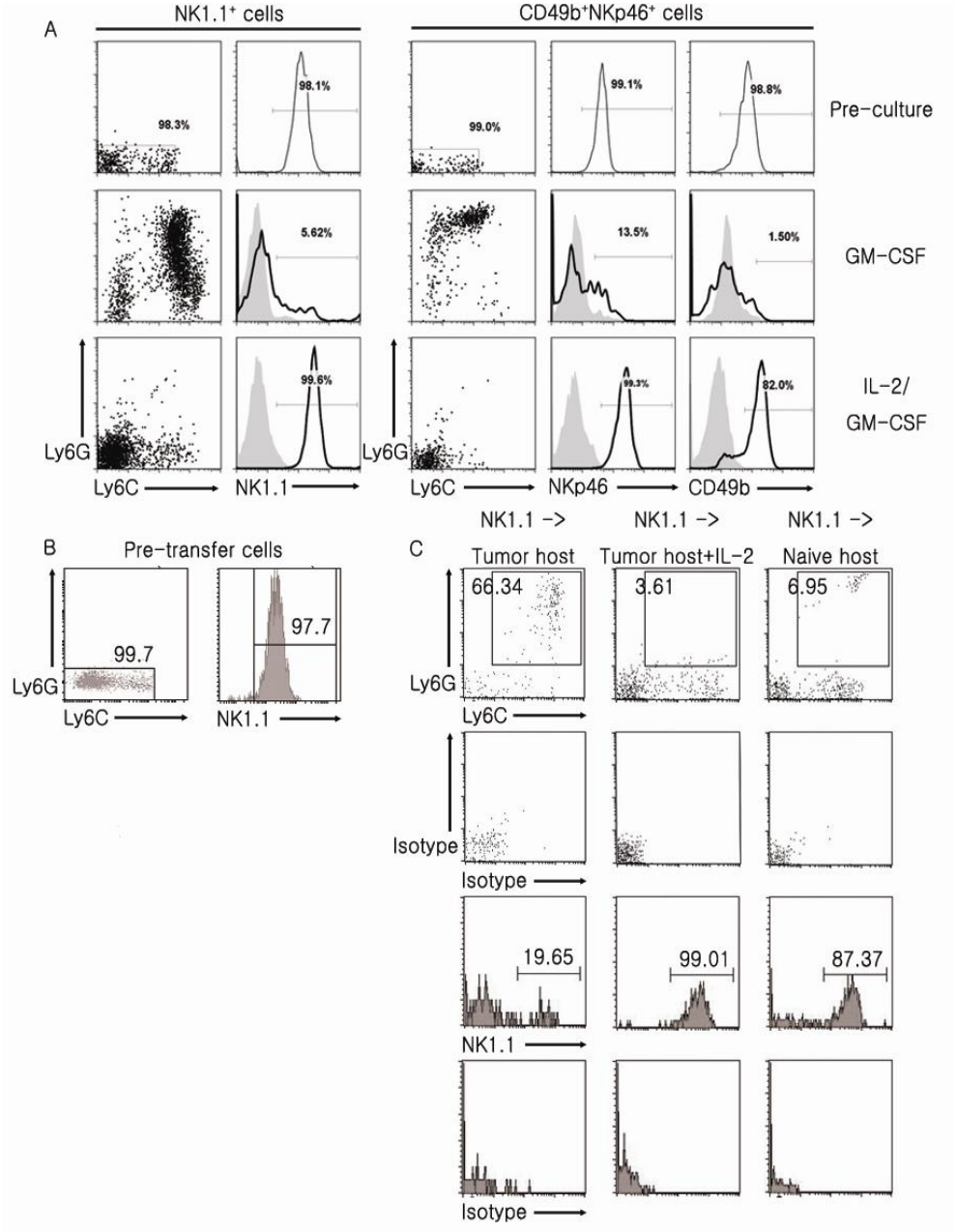

Figure 3. NK cells are converted into MDSCs.

(A) NK1.1^{+} or CD49b^{+}NKp46^{+} cells within Ly6C$^{neg/low}$ population from spleen of tumor-bearing mice were sorted and incubated with 20 ng/ml of GM-CSF or IL-2/GM-CSF. On day 5, Ly6C/G and NK marker expression were

analyzed by FACS. The numbers in the plot indicate the percentage of gated cells. The data represent 7 independent experiments. Shaded, isotype control. (B, C) $NK1.1^+$ cells were isolated from CD45.1 congenic mice inoculated s.c. with EL4 tumor cells and were transferred i.p. into CD45.2 mice. Recipient: mice injected i.p. with EL4 tumor cells 5 days before the adoptive transfer (NK1.1->Tumor host); mice injected i.p. with EL4 tumor cells 5 days before the adoptive transfer and treated with IL-2 complex daily after $NK1.1^+$ cell transfer (NK1.1->Tumor host+IL-2); and naïve mice (NK1.1->Naïve host). (C) On day 9 after the adoptive transfer, the cells were collected from the peritoneal cavity and Ly6C/G and NK1.1 expression were analyzed for $CD45.1^+CD45.2^-$ cells. The data were pooled from 3 mice per group. (B) Purity of the sorted, pre-transfer $NK1.1^+$ cells. The numbers in the plot indicate the percentage of gated cells.

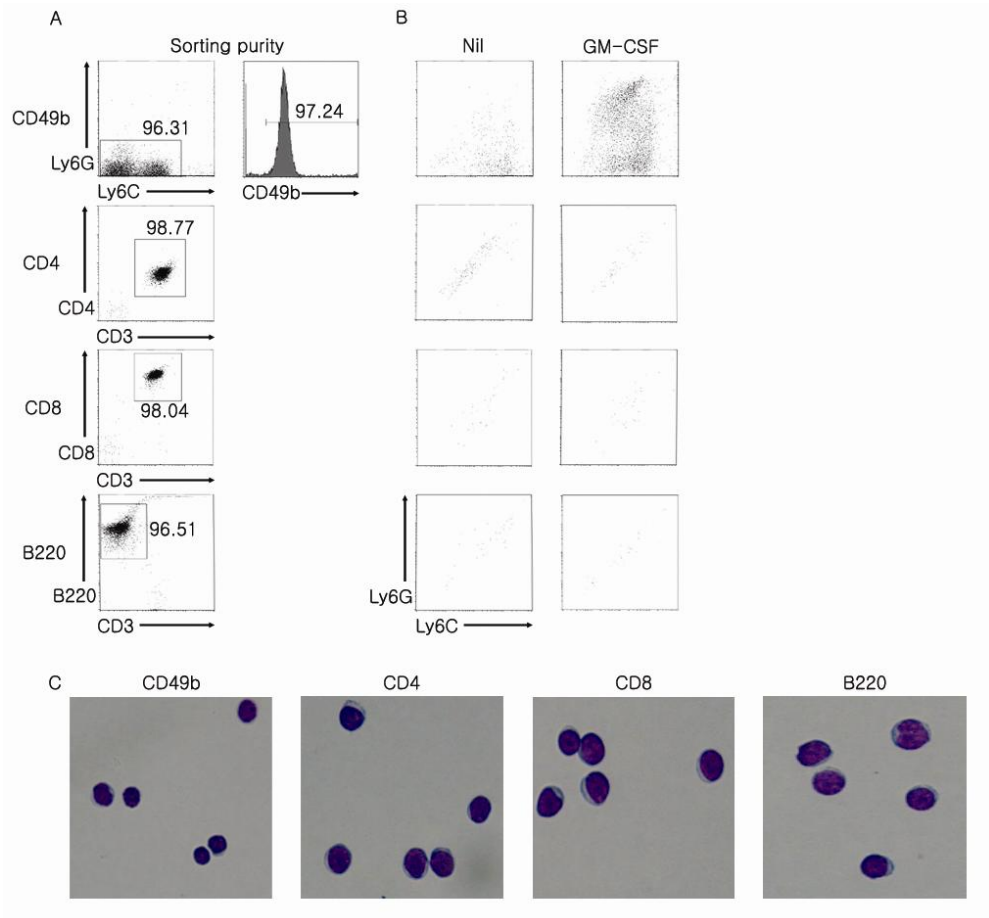

Figure 4. Only tumor CD49b$^+$ cells, not CD4$^+$ or CD8$^+$ T cells or B cells, are converted into MDSCs.

(A) CD49b$^+$, CD4$^+$, CD8$^+$ and B220$^+$ cells were purified from the tumor-bearing BALB/c mice. The numbers in the plot indicate the percentage of gated cells.

(B) Sorted cells were incubated with 20 ng/ml GM-CSF or media alone. On day 5, the cells were analyzed by FACS.

(C) Sorted cells were stained using the Diff-Quick solution. X400

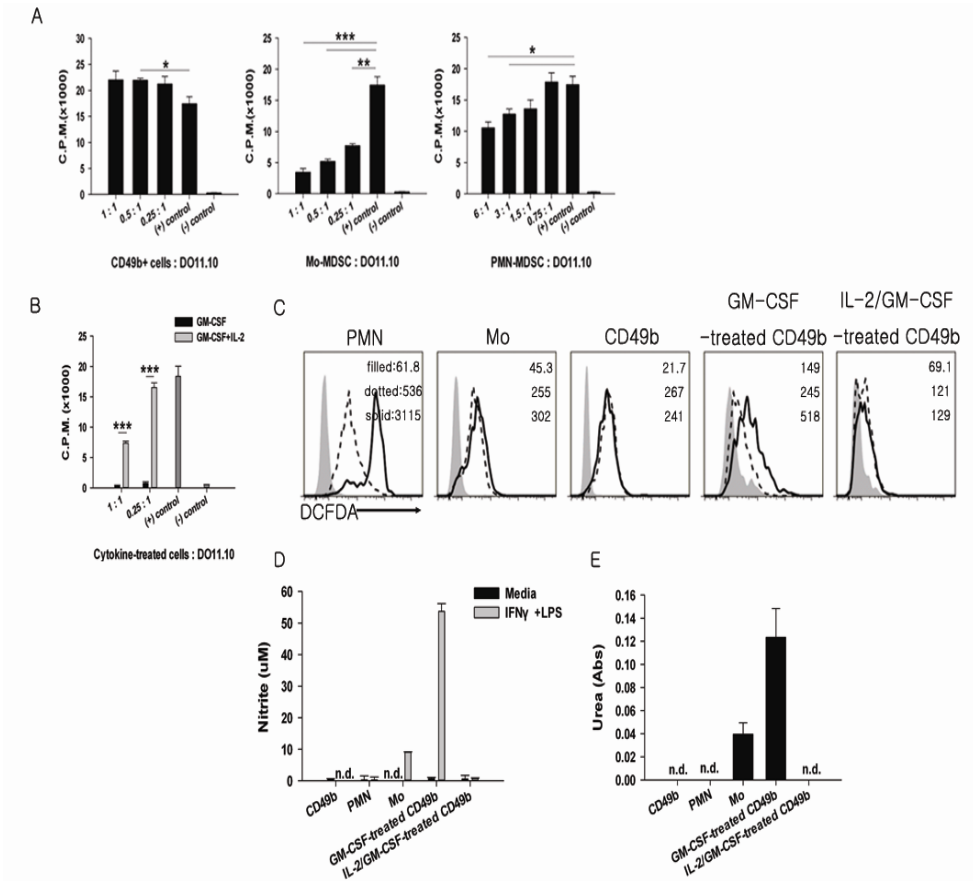

Figure 5. IL-2 reverses the suppressive activity of MDSCs converted from CD49b$^+$ cells.

Purified PMN-, Mo-MDSCs and CD49b$^+$ cells (A) or cytokine-treated CD49b$^+$ cells (B) were cocultured with DO11.10 Tg splenocytes in the presence of 250 μg/ml OVA proteins for 3 days. For the final 20-24 hr, we added 1 μCi/well [^{3}H]-thymidine. Incorporation of [^{3}H]-thymidine into the divided cells was detected using a liquid scintillation counter. (+) control, DO11.10 splenocytes + OVA proteins; (-) control, DO11.10 splenocytes alone.

The data represent the mean ± SEM. *, $P < 0.05$; **, $P < 0.01$; ***, $P < 0.001$.

(C) The level of ROS in purified $CD49b^+$, PMN- and Mo-MDSC or cytokine-treated CD49b+ cells (for 4 days, 1 day rest in media before stimulation) was measured by fluorescence intensity of DCFDA labeling after PMA stimulation for 30 min. filled, no PMA and no DCFDA; dotted, No PMA and DCFDA; solid, PMA and DCFDA.

(D, E) purified $CD49b^+$, PMN- and Mo-MDSC or cytokine-treated CD49b+ cells (for 4 days, 1 day rest in media before stimulation) were stimulated with 2 ng/ml IFN-γ and 100 ng/ml LPS for 18 h, supernatants were collected, and nitrite concentration was measured (D). arginase 1 activity (urea production) was measured in cell lysates (E).

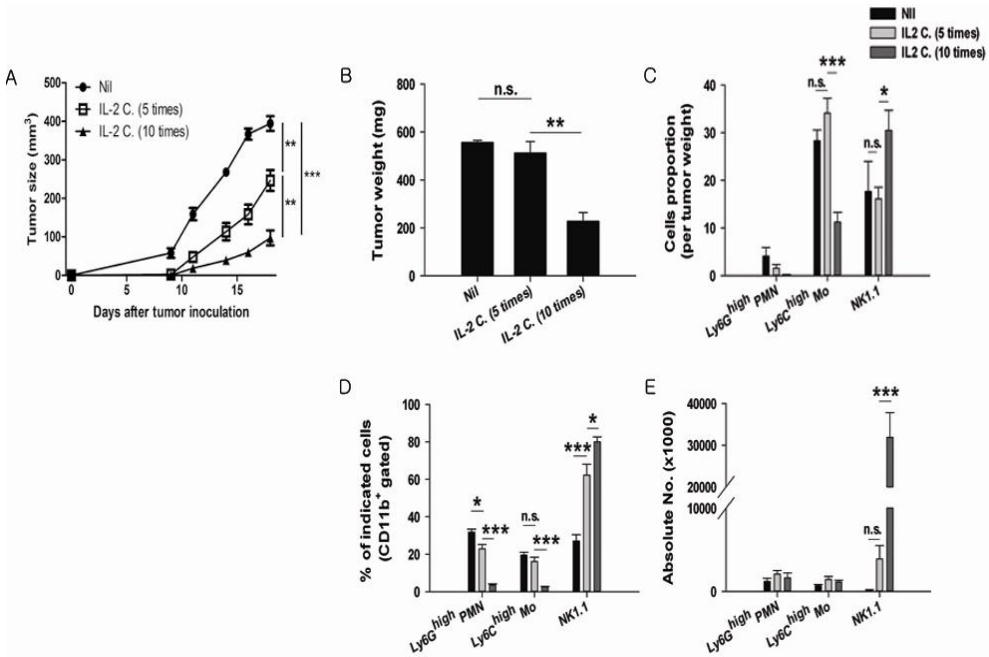

Figure 6. IL-2 subverts immunosuppressive tumor environment.

(A-E) C57BL/6 mice were injected s.c. with TC-1 tumor cells. Injection of IL-2 complex began on day 1 after tumor injection. IL-2 complex treatment was administered every other day for a total of 5 or 10 times. The volume of the implanted tumor was evaluated for 19 days following the s.c. tumor inoculation (A). At day 21 after tumor inoculation, tumor weight was measured (B) and the percentages and numbers of MDSCs and NK cells were analyzed in the tumor bed (C, %/tumor weight) and spleen (D and E). The data represent the mean ± SEM. *, $P < 0.05$; **, $P < 0.01$; ***, $P < 0.001$.

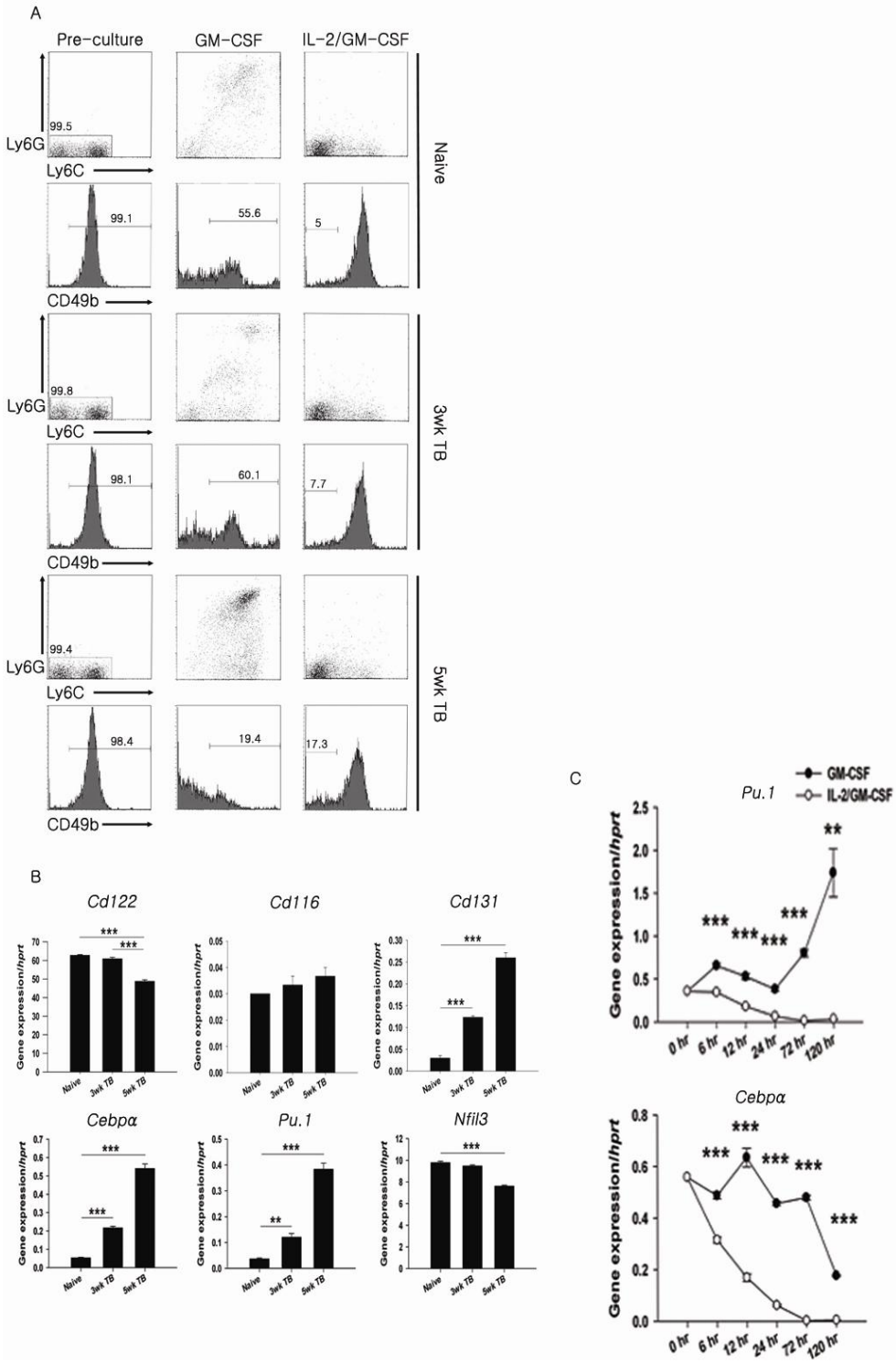

Figure 7. CD49b^{+} cells from tumor-bearing mice are more prone to

conversion into MDSCs compared to naïve CD49b$^+$ cells.

(A) CD49b$^+$ cells isolated from naïve mice and 3- and 5-week tumor-bearing mice were incubated with 20 ng/ml of the indicated cytokines. On day 5, Ly6C/G and CD49b expression were analyzed by FACS. The numbers in the plot indicate the percentage of gated cells.

(B) The expression of cytokine receptor genes in freshly isolated CD49b$^+$ cells from naïve mice and 3- and 5-week tumor-bearing mice was measured using qRT-PCR. The specific gene expression was normalized to the *Hprt* gene. The data represent the mean ± SEM.

(C) The kinetics of transcription factor expression during stimulation with GM-CSF or IL-2/GM-CSF. The data are representative of 3 independent experiments. **, $P < 0.01$; ***, $P < 0.001$.

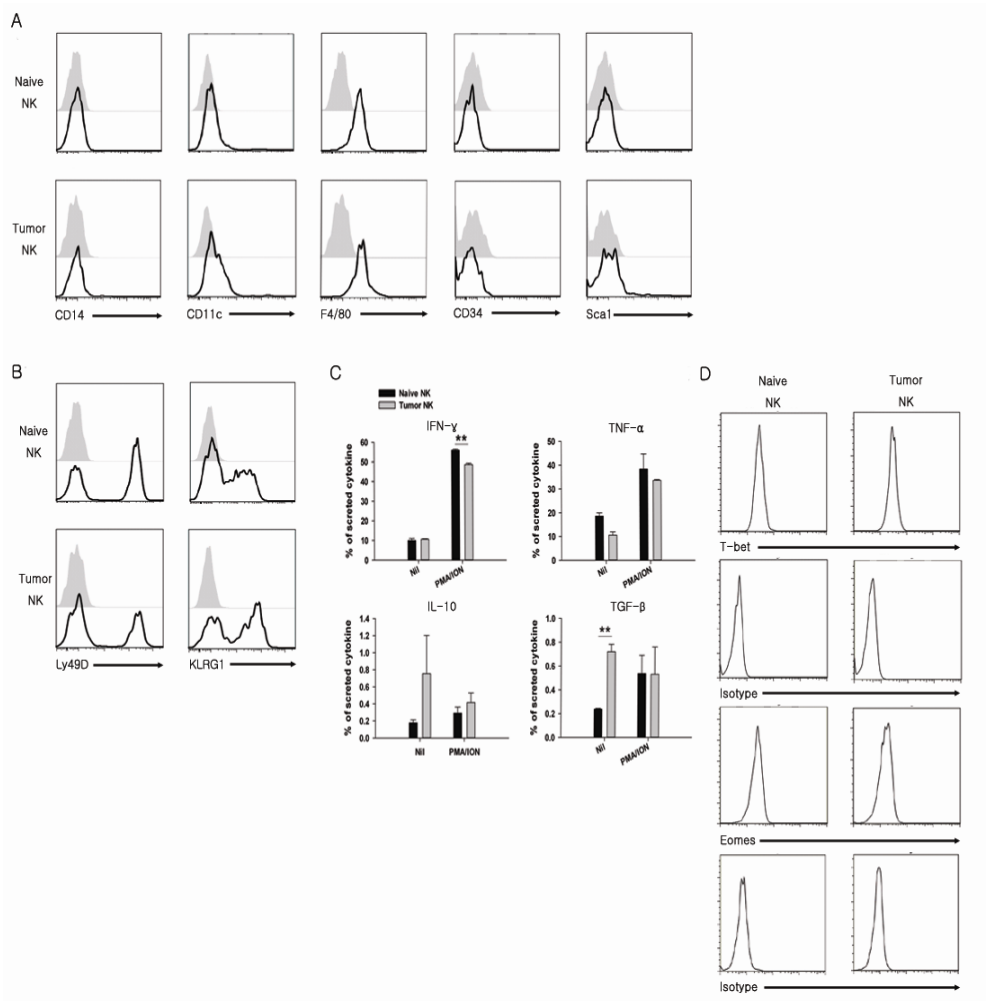

Figure 8. There is no significant difference between NK cells from naïve and tumor-bearing mice.

The expression of various markers on $Lin^-CD122^+NK1.1^+$ cells was analyzed in naïve or tumor-bearing mice. The histogram was gated for $Lin^-CD122^+NK1.1^+$ cells; lineage markers (A), NK receptors (B) and NK-cell transcription factors (D).

$Lin^-CD122^+NK1.1^+$ cells were restimulated with PMA/ION for 5 hours in the

presence of a Golgi-plug for the intracellular cytokine staining of IFN-γ, TNF-α, IL-10 and TGF-β (C).

The numbers in the plot indicate the percentage of gated cells. The data represent the mean ± SEM. **, $P < 0.01$.

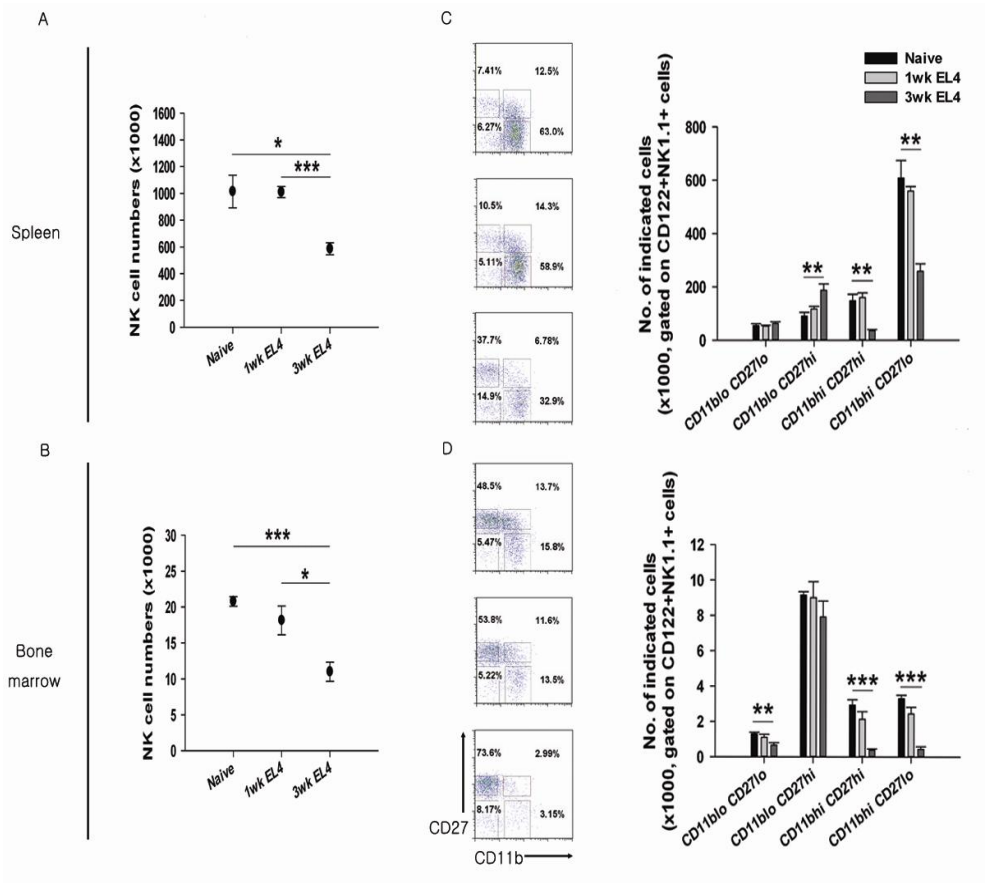

Figure 9. NK cells are decreased in tumor-bearing mice.

(A-D) C57BL/6 mice were injected s.c. with $1x10^5$ EL4 tumor cells. The mice were euthanized at 1 and 3 weeks after tumor inoculation, and the numbers of total NK cells (A and B) and the 4 maturation state populations (C and D) were analyzed in the spleen and bone marrow. NK cells are gated as Lin^- $CD122^+NK1.1^+$ cells (n=5). The numbers in the plot indicate the percentage of gated cells. The data represent the mean ± SEM. *, $P < 0.05$; **, $P < 0.01$; ***, $P < 0.001$.

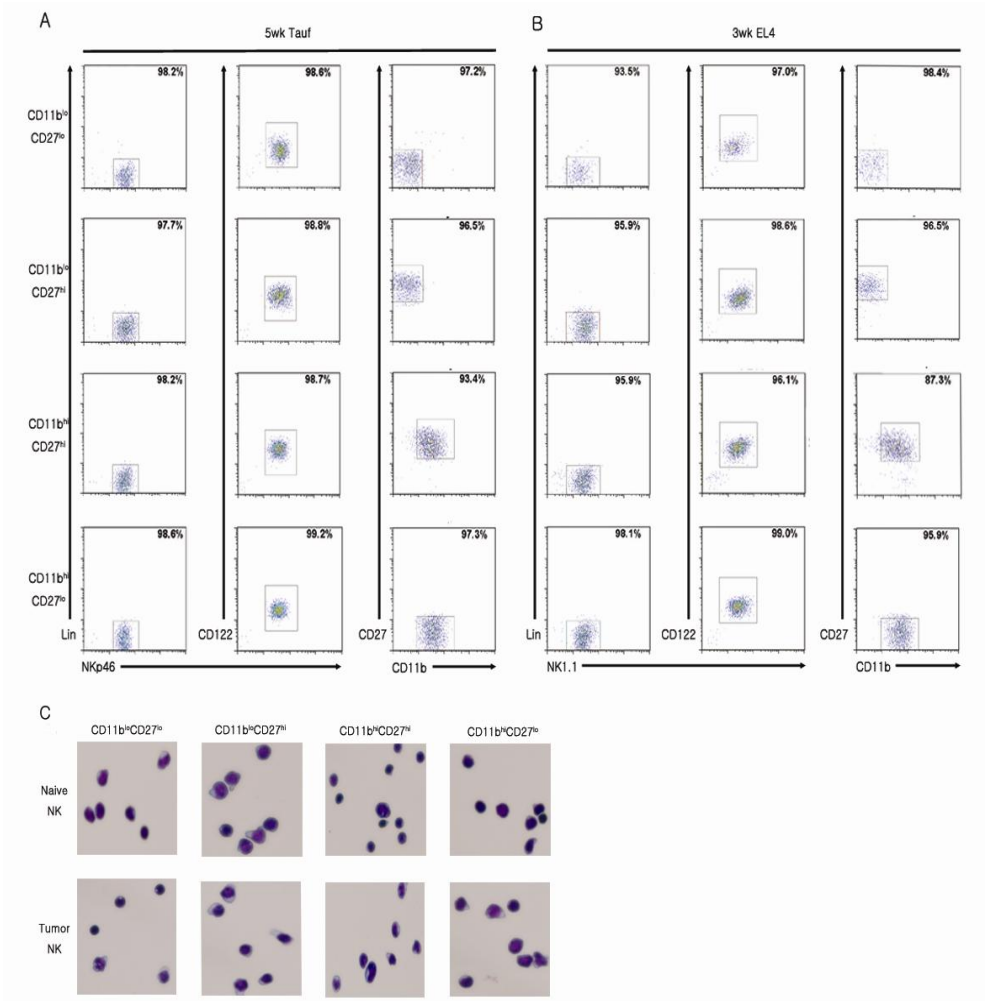

Figure 10. 4 populations of conventional NK cells divided by maturation state.

$Lin^-CD122^+NKp46^+$ (A) or $NK1.1^+$(B) cells were divided into 4 populations based on the CD11b/CD27 expression. (A, B) The sorting purity for these 4 populations is depicted.

(C) Giemsa staining of $CD11b^{low}CD27^{low}$, $CD11b^{low}CD27^{high}$, $CD11b^{high}CD27^{high}$, $CD11b^{high}CD27^{low}$ NK cells from the naïve or tumor-

bearing mice. x 400

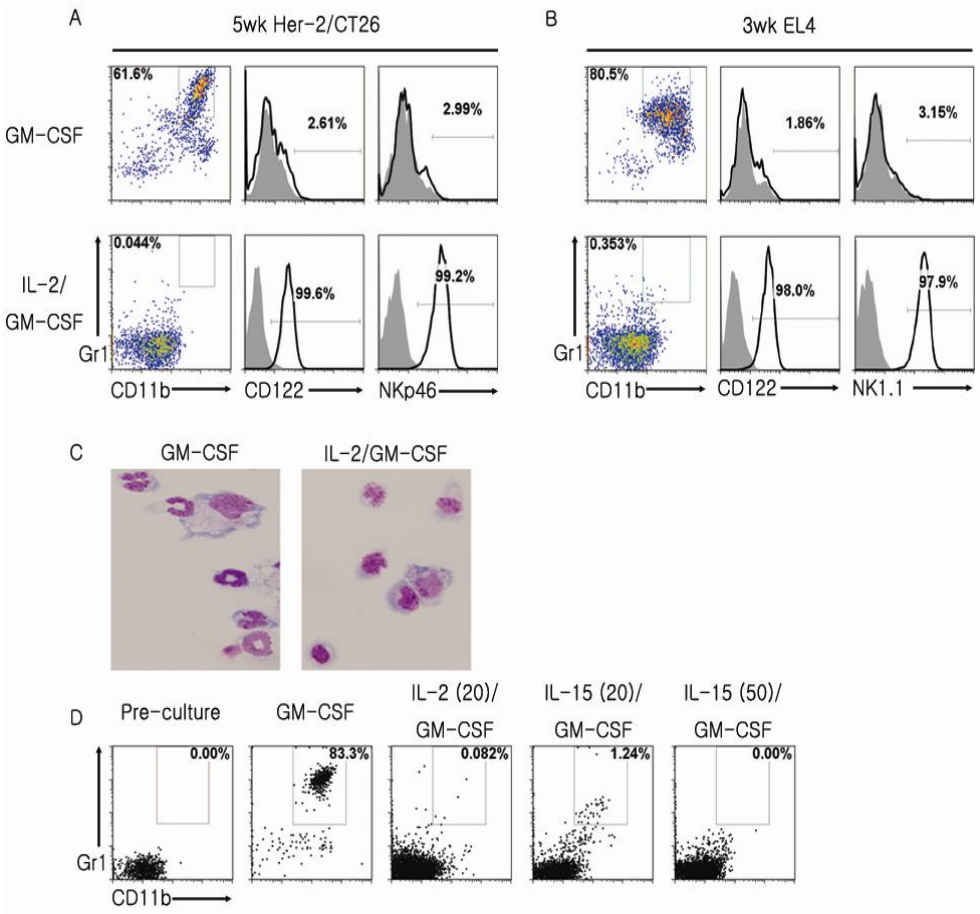

Figure 11. CD11b^{high}CD27^{high} conventional NK cells are converted into MDSCs.

Among each maturation state (CD11b^{low}CD27^{low}, CD11b^{low}CD27^{high}, CD11b^{high}CD27^{high}, CD11b^{high}CD27^{low}), Lin^{-}CD122^{+}NKp46^{+}/NK1.1^{+} CD11b^{high}CD27^{high} NK cells were sorted from tumor-bearing BALB/c (A) and C57BL/6 mice (B), respectively. Sorted cells were incubated with GM-CSF or IL-2/GM-CSF for 5 days, and Gr1^{+}CD11b^{+} cell induction and CD122, NKp46 or NK1.1 expression were analyzed (the other 3 populations of NK cells

hardly responded to the GM-CSF, data not shown). The data are representative of 3 independent experiments. Shaded, isotype control.

(C) H&E staining of $CD11b^{high}CD27^{high}$ NK cells cultured with GM-CSF or IL-2/GM-CSF for 5 days. X 400

(D) $CD11b^{high}CD27^{high}$ $NKp46^{+}$ cells from tumor-bearing mice were incubated with 20 ng/ml of GM-CSF ± IL-2 or IL-15. The numbers in the parenthesis indicate the concentration (ng/ml).

The numbers in the plot indicate the percentage of gated cells.

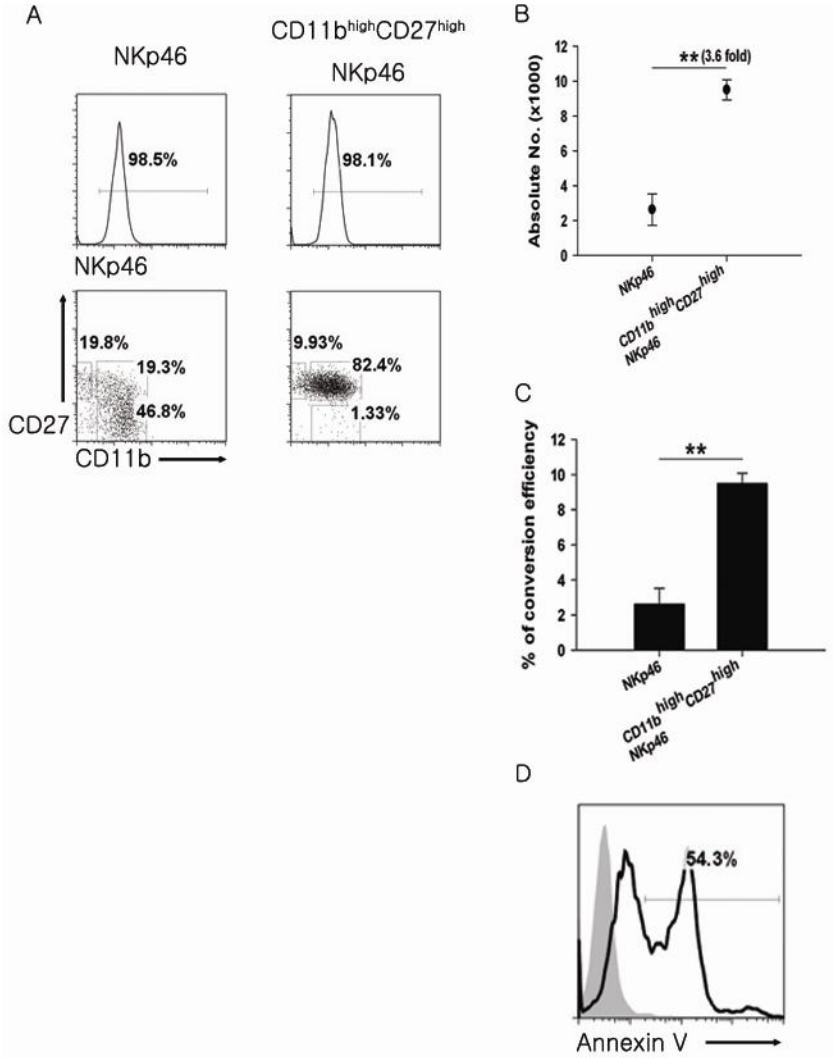

Figure 12. The efficiency of conversion is increased in CD11b^{high}CD27^{high} NKp46^{+} cells compared to NKp46^{+} total cells.

CD11b^{high}CD27^{high} NKp46^{+} cells or NKp46^{+} total cells were isolated from tumor-bearing mice (A, purity) and were incubated with GM-CSF for 5 days. The graphs indicate the number of live cells (B) and the conversion efficiency (C, live cell #/starting cell # X 100) after the incubation. (D) Annexin V

expression of GM-CSF-treated $CD11b^{high}CD27^{high}$ $NKp46^{+}$ cells was analyzed (shaded, no Annexin V staining).

The numbers in the plot indicate the percentage of gated cells. The data represent the mean ± SEM. **, $P < 0.01$. The data are representative of 2 independent experiments.

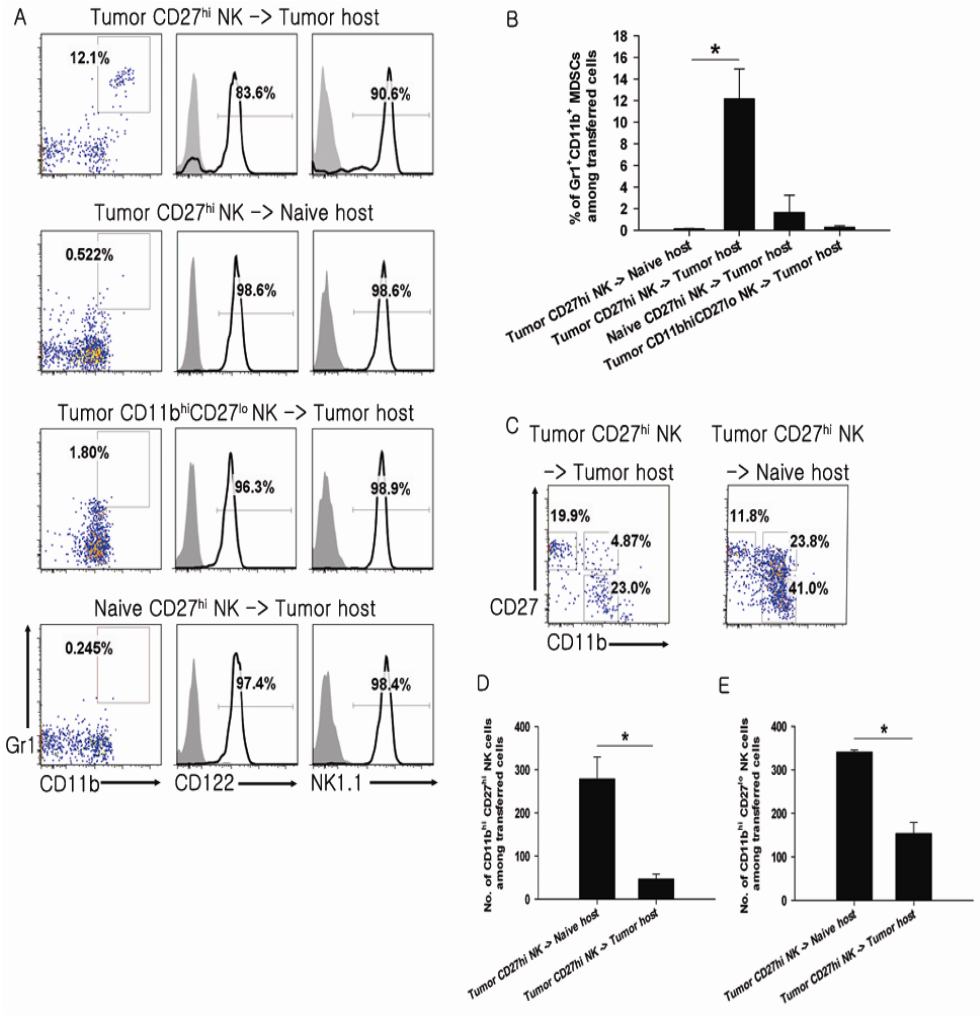

Figure 13. Conversion of CD11b^{high}CD27^{high} NK cells into MDSCs leads to CD11b^{high}CD27^{high} and CD11b^{high}CD27^{low} NK cell reduction.

The conventional NK cells from the mice that were injected s.c. with EL4 tumor cells (CD45.2 mice) were sorted and transferred into CD45.1 tumor-bearing mice. At 2 weeks post-transfer, the recipient mice were sacrificed and were analyzed for transferred cells (CD45.2^{+}CD45.1^{-}) in the spleen. (A) The

percentages of $Gr1^{+}CD11b^{+}$ MDSCs and CD122/NK1.1 expression among the transferred cells were analyzed by FACS. (B) The graph indicates the percentage of $Gr1^{+}CD11b^{+}$ MDSCs shown in A-D. (C) The maturation state of NK cells was analyzed for transferred cells ($CD45.2^{+}CD45.1^{-}$). The graphs indicate the numbers of $CD11b^{high}CD27^{high}$ (D) and $CD11b^{high}CD27^{low}$ (E) NK cells derived from the transferred cells. The data represent the mean ± SEM. The data are representative of 2 independent experiments. *, $P < 0.05$ (n=3). Shaded, isotype control.

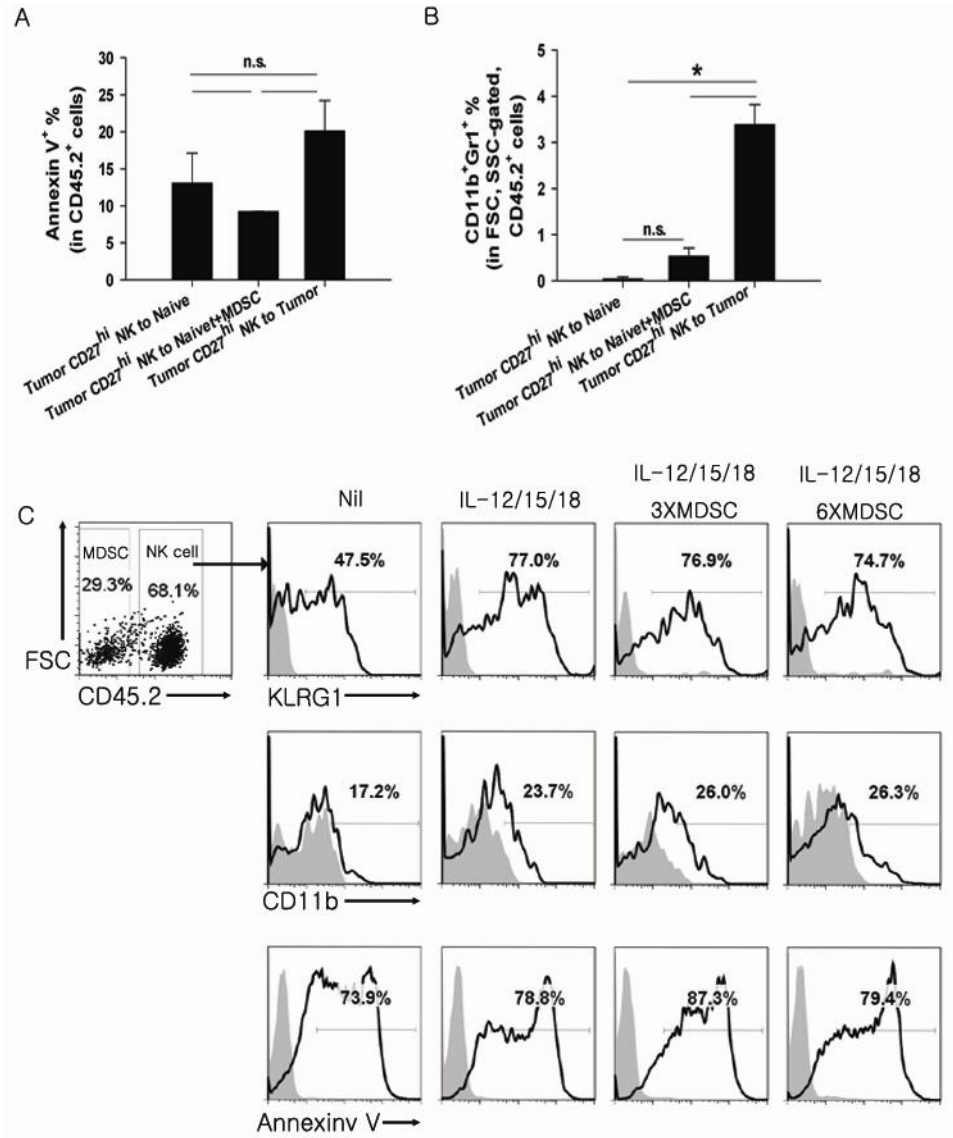

Figure 14. Endogenous MDSCs have no impact on NK cell death during the maturation course.

$CD27^{high}$ NK cells from the mice that were injected s.c. with EL4 tumor cells (CD45.2 mice) were sorted and transferred into CD45.1 naïve or tumor-bearing mice. 1 day before and after transfer, some naïve recipients were

injected i.v. with MDSCs ($4x10^6$/injection). At 1 week post-transfer, the recipient mice were sacrificed and were analyzed for transferred cells ($CD45.2^+CD45.1^-$) in the spleen. The percentages of Annexin V^+ donor cells (A) and $CD11b^+Gr1^+$ MDSCs (B) were analyzed by FACS.

(C) $CD27^{high}$ NK cells from tumor-bearing mice (CD45.2 mice) were sorted and incubated with IL-12, -15, -18 to mature those cells. To investigate the effect of MDSCs on the maturation process, $CD45.1^+$MDSCs were added 3 or 6 times and KLRG1/CD11b/Annexin V expression were analyzed. Shaded, isotype control.

The numbers in the plot indicate the percentage of gated cells. The data represent the mean ± SEM. *, $P < 0.05$ (n=2-3).

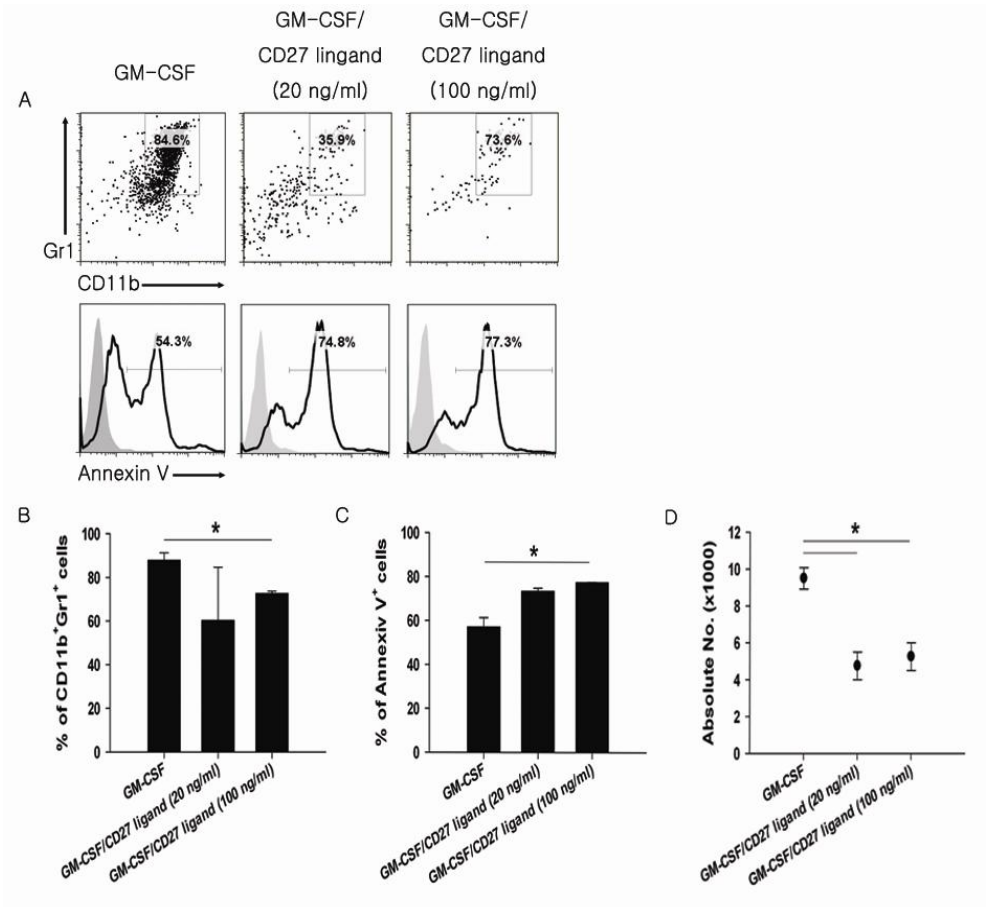

Figure 15. The conversion of CD11b^{high}CD27^{high} NK cells into MDSCs was not influenced dramatically by CD27 ligands.

CD11b^{high}CD27^{high} NK cells were isolated from tumor-bearing mice, then incubated in the presence of GM-CSF (20 ng/ml) for 5 days with or without recombinant mouse CD27 ligand (20 or 100 ng/ml). On day 5, Gr1^{+}CD11b^{+} and annexin V^{+} cells were analyzed by flow cytometry to determine the conversion and apoptosis.

The numbers in the plot indicate the percentage of gated cells. The data

represent the mean ± SEM. *, $P < 0.05$.

Discussion

The importance of NK cells for eradicating cancer cannot be overemphasized. Several studies have reported that the tumor environment impairs the development and function of NK cells [13,15] and even diminishes the number of NK cells in patients with chronic myelogenous leukemia [14]. In this study, we determined that NK cells at a specific maturation stage were converted into immunosuppressive MDSCs, a process that was impeded by IL-2 *in vitro* and *in vivo*. The inverse relationship between the percentage of $Ly6C^{neg/low}$ cells and MDSCs provided us a clue as to which NK-phenotype cells might be converted into MDSCs. This observation led us to investigate the conversion of $NKp46^{+}/NK1.1^{+}$ cells and the $Lin^{-}CD122^{+}$ conventional NK cells. It has been reported that the expression of NKp46 is restricted to NK cells and is induced in a number of minor T-cell populations, whereas myeloid cells, such as DCs, neutrophils and macrophages, do not express NKp46 [29], indicating that the conversion demonstrated in this study did not result from myeloid cells. Moreover, because NK cell maturation process proceeds sequentially as follows: $CD11b^{low}CD27^{low}$ -> $CD11b^{low}CD27^{high}$ -> $CD11b^{high}CD27^{high}$ -> $CD11b^{high}CD27^{low}$ [27], the conversion of $CD11b^{high}CD27^{high}$ NK cells into MDSCs may result in the decrease of the precursors of mature

$CD11b^{high}CD27^{low}$ NK cells, which led to a reduction of both populations, eventually giving rise to NK cell reduction in the tumor environment. A recent study showed that a particular population of $Ly6G^{+}Ly6C^{-}$ MDSCs impaired NK cell maturation in an IL-1β-4T1 tumor model [30]. However, the viability and maturation of NK cells seemed to be minimally influenced by endogenous MDSCs *in vitro* and *in vivo*, at least in EL4 tumor model, while $CD27^{high}$ NK cells were converting into MDSCs (Figure 14).

Adoptively transferred NK cells lost NK markers and converted into MDSC probably by tumor-derived GM-CSF, assumed by *in vitro* conversion assay shown in this study. Nevertheless, the conversion could be regulated by various cytokines released by tumor. We are supposed to clarify this by tumor cell knock-down experiments using shRNA or neutralization of cytokines in future studies.

Because the exact roles of CD27 in NK cell biology have not been fully investigated, it aroused our curiosity whether CD27-CD27 ligand signaling influenced NK cells or MDSCs. However, upon CD27-mediated signaling by the addition of recombinant ligands *in vitro*, no remarkable effect was found other than increased apoptosis during the conversion of NK cells into MDSCs (Figure 15), though the ligands may play other roles *in vivo*.

We demonstrated that the conversion of $Lin^{-}CD122^{+}$ conventional NK cells was prominent in only $CD11b^{high}CD27^{high}$ populations (Figure 11). 4 sorted populations of NK cells showed comparable purity for $CD122^{+}NKp46^{+}$ cells (Figure 10A), which indicates that the unwanted cells are present equally. Moreover, our morphological analysis showed that all 4 populations of NK cells isolated from tumor-bearing mice had no difference (Figure 10C). Nevertheless, NK cells in the other maturation states were not converted, indicating that this phenomenon was not because of the myeloid-biased differentiation by the tumor environment, rather NK cells in a specific maturation state were converted into MDSCs.

Several studies have endeavored to explain the development, function, migration and fate of MDSCs [31-33]. A recently published study has determined that the myeloid precursors of MDSCs that reside in the spleen are relocated to tumors [34,35]. Moreover, novel trans-differentiation pathway from monocytic to granulocytic MDSCs driven by epigenetic regulation in the tumor environment, which is beside the classical divergent development of monocytes and granulocytes, has been revealed [33]. From a different perspective, we suggest that NK-phenotype cells could be additional precursors of MDSCs. Accordingly, the precise contribution of NK cells to MDSC expansion must be

examined; however, the depletion of NK cells by antibodies did not significantly influence the accumulation of MDSCs in the tumor-bearing mice (data not shown). Apart from the question of contribution, the observation that the effector NK cells were converted into suppressor cells indicated the aggravation of the immunosuppressive environment in the tumor-bearing mice, which may also apply to cancer patients [14].

We have attempted to identify the conversion of NK cells into MDSCs in a human system. Several studies have shown that MDSCs can be produced from whole PBMCs and monocytes [36-39]. However, $CD56^+$ cells purified from the PBMCs of cancer patients were not converted into MDSCs (data not shown). These observations are consistent with the results from PBMC data in the mouse system, although the reason for this remains unclear. This indicates that the conversion of NK cells may depend on their anatomical location. Because in mice NK cells from the spleen and bone marrow and not the PBMCs were converted into MDSCs, the corresponding organs in humans should be investigated. Furthermore, the types and stages of cancer confer complexity on the environments in which NK cells are influenced by various factors, which may cause confusion when predicting the conversion of NK cells into MDSCs in the human system. Therefore, more detailed and extensive investigations of

human specimens classified by the type/stage of cancer and the organs from which NK cells are isolated will be required for future studies.

NK cells are thought to differentiate from common lymphoid progenitors (CLPs) [10,40]. However, a number of studies have debated the origin of NK cells and have shown that the cells can be derived from myeloid progenitors [41-43]. It has also been reported that common lymphoid progenitors under certain conditions and the earliest progenitors in the thymus have the potential for myeloid development [44,45]. Whether myeloid-derived NK cells exist in the periphery, and whether these cells are essential for the conversion demonstrated in this study, are intriguing issues. Even if this were the case, myeloid-derived NK cells are only a fraction of the entire NK cell population because not all of $NK1.1^{+}$ and $CD49b^{+}NKp46^{+}$ cells were converted into MDSCs; among those only $CD11b^{high}CD27^{high}$ NK cells were converted.

The levels of *Cebpα* and *Pu.1*, essential transcription factors for the development of granulocytes and monocytes [25,26], were increased in $CD49b^{+}$ cells from the tumor-bearing mice and may constitute a marker for NK cells that are converting into MDSCs. This idea was supported by the results of the kinetic study of the transcription factors; the relative expression levels of *Cebpα* and *Pu.1* were higher in GM-CSF-treated $CD49b^{+}$ cells compared with

GM-CSF/IL-2-treated cells. Several studies have reported that the ectopic expression of *Cebpα* and *Pu.1* activates trans-differentiation [46,47] and that these transcription factors synergistically program distinct responses to NF-κB activation [47], also can be induced by GM-CSF. Conversely, in the presence of IL-2, it is conceivable that STAT5 is phosphorylated and binds to target genes. We also identified the activation of STAT5 in NK cells in the presence of IL-2 by flow cytometric analysis (data not shown). It is assumed that IL-2-induced STAT5 then binds to the promoter of *Cebpα*/*Pu.1* in competition with STAT3, thereby inhibiting transcriptional and/or epigenetical regulation by STAT3 as shown by the opposing STAT3-STAT5 regulation of IL17 expression in Th17 cells [48]. The exact molecular mechanisms that regulate the conversion of these cells into MDSCs need to be investigated further.

IL-2 has been used as an immunotherapy for metastatic melanoma and metastatic renal cell carcinoma patients because of its strong stimulatory effect on $CD8^+$ T cells and NK cells [49,50]. We demonstrated that IL-2 prevented NK cells from converting into MDSCs *in vitro* and *in vivo*. However, no significant inhibitory effect on the number of MDSCs was observed in the spleen of IL-2 complex-treated tumor-bearing mice. A previous study reported that the cytokines produced from IL-2-activated NK cells prolongs the survival

of granulocytes and monocytes [22], and IL-2 complex strongly activates NK cells [18]. In this case, the effect on MDSC numbers in IL-2 complex-treated mice could be underestimated because of the increase in granulocytes/monocytes, which share surface markers, such as Ly6C, Ly6G, CD11b, with PMN- and Mo-MDSCs.

Collectively, the data in this study suggest that NK cell reduction resulted from the conversion of NK cells into MDSCs in the middle of the maturation stage, before $CD11b^{high}CD27^{high}$ NK cells give rise to the mature $CD11b^{high}CD27^{low}$ phenotype in the tumor environment. It could be a missing part of mechanisms by which results in NK cell reduction in tumor immunosuppressive environment, suggesting a novel tumor evasion mechanism. It is also noteworthy that our data suggested the possibility of conversion between lymphoid (NK cells) and myeloid cells (MDSCs) which are derived from distinct progenitor cells.

References

1. Flavell, R.A., Sanjabi, S., Wrzesinski, S.H. & Licona-Limon, P. The polarization of immune cells in the tumour environment by TGFbeta. *Nat Rev Immunol* **10**, 554-567 (2010).
2. Whiteside, T.L. The tumor microenvironment and its role in promoting tumor growth. *Oncogene* **27**, 5904-5912 (2008).
3. Zitvogel, L., Tesniere, A. & Kroemer, G. Cancer despite immunosurveillance: immunoselection and immunosubversion. *Nat Rev Immunol* **6**, 715-727 (2006).
4. Gabrilovich, D.I. & Nagaraj, S. Myeloid-derived suppressor cells as regulators of the immune system. *Nat Rev Immunol* **9**, 162-174 (2009).
5. Corzo, C.A., *et al.* HIF-1alpha regulates function and differentiation of myeloid-derived suppressor cells in the tumor microenvironment. *J Exp Med* **207**, 2439-2453 (2010).
6. Ostrand-Rosenberg, S. & Sinha, P. Myeloid-derived suppressor cells: linking inflammation and cancer. *J Immunol* **182**, 4499-4506 (2009).
7. Condamine, T. & Gabrilovich, D.I. Molecular mechanisms regulating myeloid-derived suppressor cell differentiation and function. *Trends*

Immunol **32**, 19-25 (2011).

8. Marigo, I., *et al.* Tumor-induced tolerance and immune suppression depend on the C/EBPbeta transcription factor. *Immunity* **32**, 790-802 (2010).

9. Sonda, N., Chioda, M., Zilio, S., Simonato, F. & Bronte, V. Transcription factors in myeloid-derived suppressor cell recruitment and function. *Curr Opin Immunol* **23**, 279-285 (2011).

10. Vivier, E., *et al.* Innate or adaptive immunity? The example of natural killer cells. *Science* **331**, 44-49 (2011).

11. Cerwenka, A. & Lanier, L.L. Natural killer cells, viruses and cancer. *Nat Rev Immunol* **1**, 41-49 (2001).

12. Vivier, E., Ugolini, S., Blaise, D., Chabannon, C. & Brossay, L. Targeting natural killer cells and natural killer T cells in cancer. *Nat Rev Immunol* **12**, 239-252 (2012).

13. Liu, C., *et al.* Expansion of spleen myeloid suppressor cells represses NK cell cytotoxicity in tumor-bearing host. *Blood* **109**, 4336-4342 (2007).

14. Pierson, B.A. & Miller, J.S. CD56+bright and CD56+dim natural killer cells in patients with chronic myelogenous leukemia progressively

decrease in number, respond less to stimuli that recruit clonogenic natural killer cells, and exhibit decreased proliferation on a per cell basis. *Blood* **88**, 2279-2287 (1996).

15. Sibbitt, W.L., Jr., *et al.* Defects in natural killer cell activity and interferon response in human lung carcinoma and malignant melanoma. *Cancer Res* **44**, 852-856 (1984).

16. Chang, S.Y., Lee, K.C., Ko, S.Y., Ko, H.J. & Kang, C.Y. Enhanced efficacy of DNA vaccination against Her-2/neu tumor antigen by genetic adjuvants. *Int J Cancer* **111**, 86-95 (2004).

17. Chung, Y., *et al.* CD1d-restricted T cells license B cells to generate long-lasting cytotoxic antitumor immunity in vivo. *Cancer Res* **66**, 6843-6850 (2006).

18. Boyman, O., Kovar, M., Rubinstein, M.P., Surh, C.D. & Sprent, J. Selective stimulation of T cell subsets with antibody-cytokine immune complexes. *Science* **311**, 1924-1927 (2006).

19. Letourneau, S., *et al.* IL-2/anti-IL-2 antibody complexes show strong biological activity by avoiding interaction with IL-2 receptor alpha subunit CD25. *Proc Natl Acad Sci U S A* **107**, 2171-2176 (2010).

20. Akgul, C., Moulding, D.A. & Edwards, S.W. Molecular control of

neutrophil apoptosis. *FEBS Lett* **487**, 318-322 (2001).

21. Heidenreich, S. Monocyte CD14: a multifunctional receptor engaged in apoptosis from both sides. *J Leukoc Biol* **65**, 737-743 (1999).

22. Bhatnagar, N., *et al.* Cytokine-activated NK cells inhibit PMN apoptosis and preserve their functional capacity. *Blood* **116**, 1308-1316 (2010).

23. Di Santo, J.P. Natural killer cell developmental pathways: a question of balance. *Annu Rev Immunol* **24**, 257-286 (2006).

24. Ramirez, K. & Kee, B.L. Multiple hats for natural killers. *Curr Opin Immunol* **22**, 193-198 (2010).

25. Ceredig, R., Rolink, A.G. & Brown, G. Models of haematopoiesis: seeing the wood for the trees. *Nat Rev Immunol* **9**, 293-300 (2009).

26. Iwasaki, H. & Akashi, K. Myeloid lineage commitment from the hematopoietic stem cell. *Immunity* **26**, 726-740 (2007).

27. Chiossone, L., *et al.* Maturation of mouse NK cells is a 4-stage developmental program. *Blood* **113**, 5488-5496 (2009).

28. Ni, J., Miller, M., Stojanovic, A., Garbi, N. & Cerwenka, A. Sustained effector function of IL-12/15/18-preactivated NK cells against established tumors. *J Exp Med* **209**, 2351-2365 (2012).

29. Narni-Mancinelli, E., *et al.* Fate mapping analysis of lymphoid cells expressing the NKp46 cell surface receptor. *Proc Natl Acad Sci U S A* **108**, 18324-18329 (2011).

30. Elkabets, M., *et al.* IL-1beta regulates a novel myeloid-derived suppressor cell subset that impairs NK cell development and function. *Eur J Immunol* **40**, 3347-3357 (2010).

31. Cheng, P., *et al.* Inhibition of dendritic cell differentiation and accumulation of myeloid-derived suppressor cells in cancer is regulated by S100A9 protein. *J Exp Med* **205**, 2235-2249 (2008).

32. Ma, G., *et al.* Paired immunoglobin-like receptor-B regulates the suppressive function and fate of myeloid-derived suppressor cells. *Immunity* **34**, 385-395 (2011).

33. Youn, J.I., *et al.* Epigenetic silencing of retinoblastoma gene regulates pathologic differentiation of myeloid cells in cancer. *Nat Immunol* **14**, 211-220 (2013).

34. Cortez-Retamozo, V., *et al.* Origins of tumor-associated macrophages and neutrophils. *Proc Natl Acad Sci U S A* **109**, 2491-2496 (2012).

35. Bayne, L.J., *et al.* Tumor-derived granulocyte-macrophage colony-stimulating factor regulates myeloid inflammation and T cell immunity

in pancreatic cancer. *Cancer Cell* **21**, 822-835 (2012).

36. Lechner, M.G., Liebertz, D.J. & Epstein, A.L. Characterization of cytokine-induced myeloid-derived suppressor cells from normal human peripheral blood mononuclear cells. *J Immunol* **185**, 2273-2284 (2010).

37. Lechner, M.G., *et al.* Functional characterization of human Cd33+ and Cd11b+ myeloid-derived suppressor cell subsets induced from peripheral blood mononuclear cells co-cultured with a diverse set of human tumor cell lines. *J Transl Med* **9**, 90 (2011).

38. Obermajer, N. & Kalinski, P. Generation of myeloid-derived suppressor cells using prostaglandin E2. *Transplant Res* **1**, 15 (2012).

39. Obermajer, N., Muthuswamy, R., Lesnock, J., Edwards, R.P. & Kalinski, P. Positive feedback between PGE2 and COX2 redirects the differentiation of human dendritic cells toward stable myeloid-derived suppressor cells. *Blood* **118**, 5498-5505 (2011).

40. Kondo, M., Weissman, I.L. & Akashi, K. Identification of clonogenic common lymphoid progenitors in mouse bone marrow. *Cell* **91**, 661-672 (1997).

41. Grzywacz, B., Kataria, N., Blazar, B.R., Miller, J.S. & Verneris, M.R.

Natural killer-cell differentiation by myeloid progenitors. *Blood* **117**, 3548-3558 (2011).

42. Marquez, C., *et al.* Identification of a common developmental pathway for thymic natural killer cells and dendritic cells. *Blood* **91**, 2760-2771 (1998).

43. Perez, S.A., *et al.* A novel myeloid-like NK cell progenitor in human umbilical cord blood. *Blood* **101**, 3444-3450 (2003).

44. Kondo, M., *et al.* Cell-fate conversion of lymphoid-committed progenitors by instructive actions of cytokines. *Nature* **407**, 383-386 (2000).

45. Luc, S., *et al.* The earliest thymic T cell progenitors sustain B cell and myeloid lineage potential. *Nat Immunol* **13**, 412-419 (2012).

46. Ghisletti, S., *et al.* Identification and characterization of enhancers controlling the inflammatory gene expression program in macrophages. *Immunity* **32**, 317-328 (2010).

47. Jin, F., Li, Y., Ren, B. & Natarajan, R. PU.1 and C/EBP(alpha) synergistically program distinct response to NF-kappaB activation through establishing monocyte specific enhancers. *Proc Natl Acad Sci U S A* **108**, 5290-5295 (2011).

48. Yang, X.P., *et al.* Opposing regulation of the locus encoding IL-17 through direct, reciprocal actions of STAT3 and STAT5. *Nat Immunol* **12**, 247-254 (2011).

49. Klapper, J.A., *et al.* High-dose interleukin-2 for the treatment of metastatic renal cell carcinoma : a retrospective analysis of response and survival in patients treated in the surgery branch at the National Cancer Institute between 1986 and 2006. *Cancer* **113**, 293-301 (2008).

50. Rosenberg, S.A., *et al.* Treatment of 283 consecutive patients with metastatic melanoma or renal cell cancer using high-dose bolus interleukin 2. *JAMA* **271**, 907-913 (1994).

국문 초록

자연 살해 세포 (natural killer cells)는 암으로부터 신체를 지키는 중요한 효과기 세포 중 하나이다. 자연 살해 세포의 수 및 기능의 유지는 암 형성에 대한 장벽으로 작용하고, 암 환자에 있어서 좋은 예후를 초래함이 잘 알려져 있다. 반면에, 미분화 골수성 세포 (myeloid-derived suppressor cells)는 암 환경에서 축적되는 다양한 미성숙 골수성 세포의 집합으로, 면역 감시 체계를 전복시키고 암의 진행을 촉진시킴이 밝혀졌다. 미분화 골수성 세포의 기능의 특성 및 운명에 대한 연구는 잘 되어 있는 반면, 암 환경에서의 이들의 분화 과정에 대한 연구는 미진한 상태이다. 이번 연구에서는, 암 성장이 진행됨에 따른 세포 분포 비율 변화 관찰을 통해 미분화 골수성 세포의 전구 세포를 규명하고자 하였다. 이를 위해 비장 내 $CD11b^{+}$ 세포 중 Ly6C, Ly6G 발현 정도에 따른 세포 분포를 관찰하였고, 이 때 $Ly6C^{high}$ 또는 $Ly6G^{high}$ 표현형의 미분화 골수성 세포는 점점 증가하는 반면 $Ly6C^{neg/low}$ 세포는 감소함을 확인하였다. 본인은 이러한 결과가 암 환경에서 $Ly6c^{neg/low}$ 세포가 미분화 골수성 세포로 변하기 때문에 초래된 것이라 가설을 세우고, 이를 검증하기 위해 초고속 유세포 분리기를 이용하여 고순도로 $Ly6c^{neg/low}$ 세포를 분리한 후 미분화 골수성 세포 축적과 관련 있다고 알려진 다양한 싸이토카인과

체외 배양하였고, 그 결과 이들이 미분화 골수성 세포의 전구 세포임을 확인하였다. 그리고 Ly6c$^{neg/low}$ 세포 분포를 이루는 세포들의 정체성을 확인하는 과정에서 자연 살해 세포가 미분화 골수성 세포로 변함을 최초로 확인할 수 있었다. 자연 살해 세포는 CD11b/CD27 발현 정도에 따라 4 단계의 성숙 단계 (CD11b^{low}CD27^{low}, CD11b^{low}CD27^{high}, CD11b^{high}CD27^{high}, CD11b^{high}CD27^{low})로 나뉘어 지고, 이 중 암을 가진 마우스의 CD11b^{high}CD27^{high} 자연 살해 세포가 미분화 골수성 세포로 변하여 자연 살해 세포 결핍을 초래함을 체외 및 체내 실험을 통해 확인하였다. 하지만 자연 살해 세포 활성화 싸이토카인인 IL-2가 자연 살해 세포의 미분화 골수성 세포로의 변화를 억제하고 원래의 표현형을 유지시키고, 뿐 만 아니라 세포 독성 T 세포 (cytotoxic T lymphocyte)를 활성화 시켜 항암 치료 효과를 유도함을 밝혔다. 본 연구를 통해 암의 면역 체계의 회피에 대한 새로운 현상을 밝혔고, 이를 통해 암 면역 치료를 위한 효과적인 전략에 대해 새로운 방법을 제시할 수 있을 것으로 기대할 수 있다.

주요어 : 자연 살해 세포, 미분화 골수성 세포, 암 환경, IL-2, 세포 독성 T 세포, CD11b, CD27, 초고속 유세포 분리기

학 번 : 2006-23438